AGSO Journal of Australian Geology & Geophysics, 15 (2), 191–215

Diagenesis of Jurassic and Lower Cretaceous sandstones of the Eromanga Basin in New South Wales

Fuxiang He[1] & Patrick J. Conaghan[1]

The Jurassic and Lower Cretaceous sandstones of the Eromanga Basin in New South Wales can be divided into quartzose and volcanolithic petrofacies. The latter comprises sandstones of the Cadna-owie and Wallumbilla Formations which are predominantly volcanic-orogen-sourced lacustrine-to-paralic and shallow-marine deposits; the quartzose petrofacies comprises the craton-sourced fluvial Hooray Sandstone, the correlative fluvial and lacustrine Mooga Formation, and subordinate basal and other intercalated phases of the overlying Cadna-owie Formation. The diagenetic overprints in the sandstones include physical compaction, clay infiltration, cementation, and the dissolution and replacement of labile grains. The authigenic minerals in the chemically reactive volcanolithic sandstones are, in temporal order of appearance: syndepositional-glauconie, pyrite, sporadic carbonate, smectite (including nontronite, smectite and mixed-layers mectite/chlorite), zeolite (heulandite and mordenite), and kaolinite; and in the chemically stable quartzose sandstones, the authigenic minerals are, in order of appearance: quartz (phase I), sporadic carbonate, accessory chlorite, and quartz (phase II) and kaolinite. Cutans of mechanically infiltrated clay and/or thin authigenic chlorite grain-coatings constitute early diagenetic overprints in the quartzose sandstones of the Hooray Sandstone/Mooga Formation and the Cadna-owie Formation, and thereby minimised subsequent reduction of the substantial primary porosity of these rocks by precluding pervasive quartz-overgrowth cementation. The present-day excellent aquifer function of these quartzose sandstones is due largely to this circumstance, perhaps augmented by a history of geochemical pore-fluid conditions that were generally unfavourable for the volumetrically large-scale precipitation of either silica or carbonate.

The volcanolithic sandstones average 35% core porosity and 125 md permeability. Micropores constitute the predominant pore-type in these rocks and, where macropores are present, they comprise both isolated primary intergranular and secondary grain-dissolution pores, the origin of the latter likely being related to the interaction between labile sand grains and pore-fluid derived in part from intercalated organic-rich mudrocks. The quartzose sandstone has 29% (mean) core porosity and 676 md (mean) permeability; and the pore-types are mainly primary intergranular pores, and accessory intragranular grain-dissolution pores (mostly within feldspar grains). The development of the secondary-dissolution pores in the quartzose sandstone manifests the influence of meteoric (artesian) water and is a late diagenetic event. The distribution patterns of porosity–permeability of the lithic and quartzose sandstones correlate well with the respective depositional environments of these rocks as manifested by their bulk lithofacies characteristics.

Introduction

The Jurassic and Early Cretaceous Eromanga Basin together with the Surat, Clarence–Moreton and Carpentaria Basins form the Great Australian Basin in eastern Australia, covering an area of 1.7 x 10^6 km^2 in the states of Queensland, South Australia, New South Wales (NSW), and the Northern Territory (Fig. 1). Tectonically, the Eromanga Basin developed as a broad intracratonic downwarp of uncertain origin (Moore et al., 1986; Gallagher, 1990); but in relation to the coeval volcanic arc situated along the convergent northeastern continental margin of Australia, the Eromanga Basin developed in a backarc setting and has been interpreted as an epicratonic basin (Jones & Veevers, 1983). The Eromanga Basin succession attains a maximum thickness of about 3 km in Queensland and South Australia, and consists of Jurassic fluvial and lacustrine sediments and Lower Cretaceous sediments of fluvial through lacustrine to paralic and shallow-marine origins.

In NSW, the Eromanga Basin succession is relatively thin, the maximum thickness of about 1 km being developed in the northwest corner of the state (Fig. 2). The succession mainly comprises the upper Jurassic to Lower Cretaceous fluvial and lacustrine Hooray Sandstone/Mooga Formation and the overlying lacustrine-to-paralic and shallow-marine Cadna-owie and Wallumbilla Formations (Fig. 3). Middle to Upper Jurassic rocks of the Injune Creek Group probably exist as thin discontinous bodies of sediment between the Hooray Sandstone and basement rock in the northwestern corner of NSW (Hawke & Bourke, 1984, p.94; Alder, 1993), but no core is available from this unit. Additionally, the Middle Jurassic Hutton Sandstone appears to be absent in the NSW part of the Eromanga Basin (Hawke & Bourke, 1984, p.94). Uppermost Albian and Cenomanian rocks of the upper part of the Rolling Downs Group (i.e. Toolebuc Formation, Allaru Mudstone, and Winton Formation) are developed in the northwestern part of the study area (Figs 2,3) and are dominated by mudrocks.

Provenance studies of the Eromanga Basin succession in NSW (He, 1992) suggest that the volcanolithic sandstones of the Wallumbilla and Cadna-owie Formations, which contain abundant andesitic volcanic rock-fragments (VRFs), were derived mainly from a coeval volcanic orogen located along the northeastern continental margin of Australia (Jones & Veevers, 1983); the quartzose Hooray Sandstone/Mooga Formation and quartzose intercalations and phyllarenitic basal phases of the Cadna-owie Formation were sourced from plutonic and metamorphic basement rocks and possibly older sedimentary successions flanking the basin on the west and south.

This paper documents diagenetic characteristics and porosity–permeability distributions of sandstones of the Wallumbilla and Cadna-owie Formations and the Hooray Sandstone/Mooga Formation in the NSW portion of the Eromanga Basin, and assesses the likely geological factors involved in the post-depositional evolution of these sediments. As such, this work complements similar studies of potential or actual reservoir rocks of the Eromanga Basin succession (or parts thereof) in adjoining areas of South Australia and Queensland (e.g. Ambrose et al., 1982; Wall, 1987; Duff, 1987; Green et al., 1989) and of the Surat Basin succession (or parts thereof) in NSW (Arditto, 1982, 1983) and Queensland (Hawlader, 1990a,b).

[1] School of Earth Sciences, Macquarie University, NSW 2109 Australia.

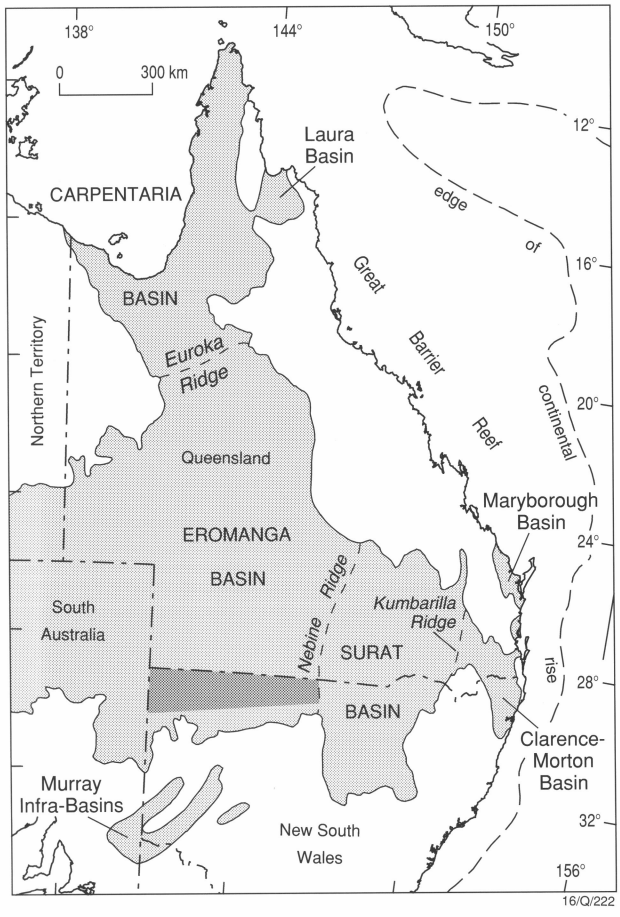

Figure 1. Location of the Great Australian Basin and associated areas (stippled) of Jurassic–Cretaceous sedimentation in eastern Australia (modified from Doutch & Wilford, 1981); the study area is highlighted and further detailed in Figure 2.

Methodology

Diagenesis of the Eromanga Basin sandstones was studied by integration of petrographic and porosity and permeability data. One hundred and twenty-five sandstone samples were selected from cores of six stratigraphic test wells and one petroleum exploration well along a west–east transect (Fig. 2). Ninety-four porosity and permeability measurements were made on petrophysical core-plugs extracted from the primary core of the sampled intervals. Most of these measurements were made by P.G. Duff of the Core and Cuttings Laboratory of the Bureau of Resource Sciences in Canberra, using air and dry nitrogen as the saturating and flowing media, respectively. Additional porosity and permeability measurements were undertaken by the authors using helium and air as the saturating and flowing media, respectively. All permeability values reported here refer to horizontal permeability. One hundred and twenty-five petrographic thin-sections were prepared from the surrounds of the petrophysical core-plugs, and in the case where such surrounds are not available, a thin-section was cut from one of the couplet of core-plugs (i.e. horizontal and vertical) that had been made from each sample of primary core. Kerosene was used as the cutting and grinding lubricant in the case of labile samples, and the samples were impregnated with blue epoxy resin to distinguish natural porosity from artificial pore-spaces. Quantitative data of the sandstone mineralogy and types of pore-spaces were obtained by the point-counting method using a standard count of 1000 points per slide (Table 1). Thin-sections with carbonate cements were stained with K-ferricyanide and alizarin red-S to differentiate the various carbonate minerals present. The identification of feldspars was facilitated by staining techniques (cf. Boone & Wheeler, 1968), using Na-cobaltinitrite for K-feldspars (yellow stain) and amaranth for plagioclase (pink stain). Compositions of detrital feldspars in four representative samples were further analysed by electron microprobe. Scanning-electron microscope (SEM) analysis was carried out on many samples to study the authigenic minerals, and the texture and pore-types of these sandstones; SEM specimens were coated with both carbon and gold. Energy dispersive X-ray (EDX) analysis was employed to study the compositions of representative authigenic minerals. X-ray diffraction (XRD) analysis of the oriented clay-fraction (<2 μm) was carried out on nine representative samples. The distribution of macropores and micropores in four representative samples from DM Bellfield 1A was further investigated by the mercury injection technique.

Table 1. Categories of sandstone constituents used in the point-counting analysis. Matrix terminology is that of Dickinson (1970).

Detrital mode	
	Quartz (Q) = plutonic/metamorphic + vein + volcanic
	Feldspar (F) = plagioclase + K-feldspar
	Lithic fragments (L) = volcanic + metamorphic + sedimentary
Other detritus (mica, heavy minerals)	
Pore-fillings	
	Non-phyllosilicate cements (quartz, carbonate, feldspar, zeolite, etc.)
	Epimatrix and phyllosilicate cements (smectite, illite, kaolinite, chlorite, etc.)
	Orthomatrix
Macropores	
	Primary (intergranular, intragranular)
	Secondary (intergranular, intragranular, fracture)

Detrital minerals

Sandstones of the Wallumbilla Formation and most of the Cadna-owie Formation are predominantly volcanolithic (i.e. detrital quartz content <50 whole-rock%, and Lv>Lm), ranging from feldspathic litharenite to litharenite (Figs 3,4; terminology of Folk et al., 1970). However, phases of quartzose and sublithic sandstone (i.e. detrital quartz >50 whole-rock%) occur at the base of and intercalated within the Cadna-owie Formation, particularly in the western part of the Eromanga Basin in NSW (i.e. in Lake Stewart 1). The predominantly quartzose Hooray Sandstone/Mooga Formation ranges from sublitharenite through subfeldsarenite to quartzarenite (Fig. 4A), and its basal part in particular is phyllarenitic in some wells (e.g. Weilmoringle 1A) reflecting local provenance from underlying and/or adjacent areas of metamorphic basement rocks. From east to west along the transect (Fig. 2), sandstones of all formations become progressively more quartzose (He, 1992, his fig. 2.1c-e).

At the gross formation/petrofacies level, detrital quartz comprises 35.0% and 90.2% (means) in the volcanolithic and quartzose sandstones, respectively (Table 2). Most quartz grains were identified as common monocrystalline quartz of plutonic or metamorphic origin, but polycrys-

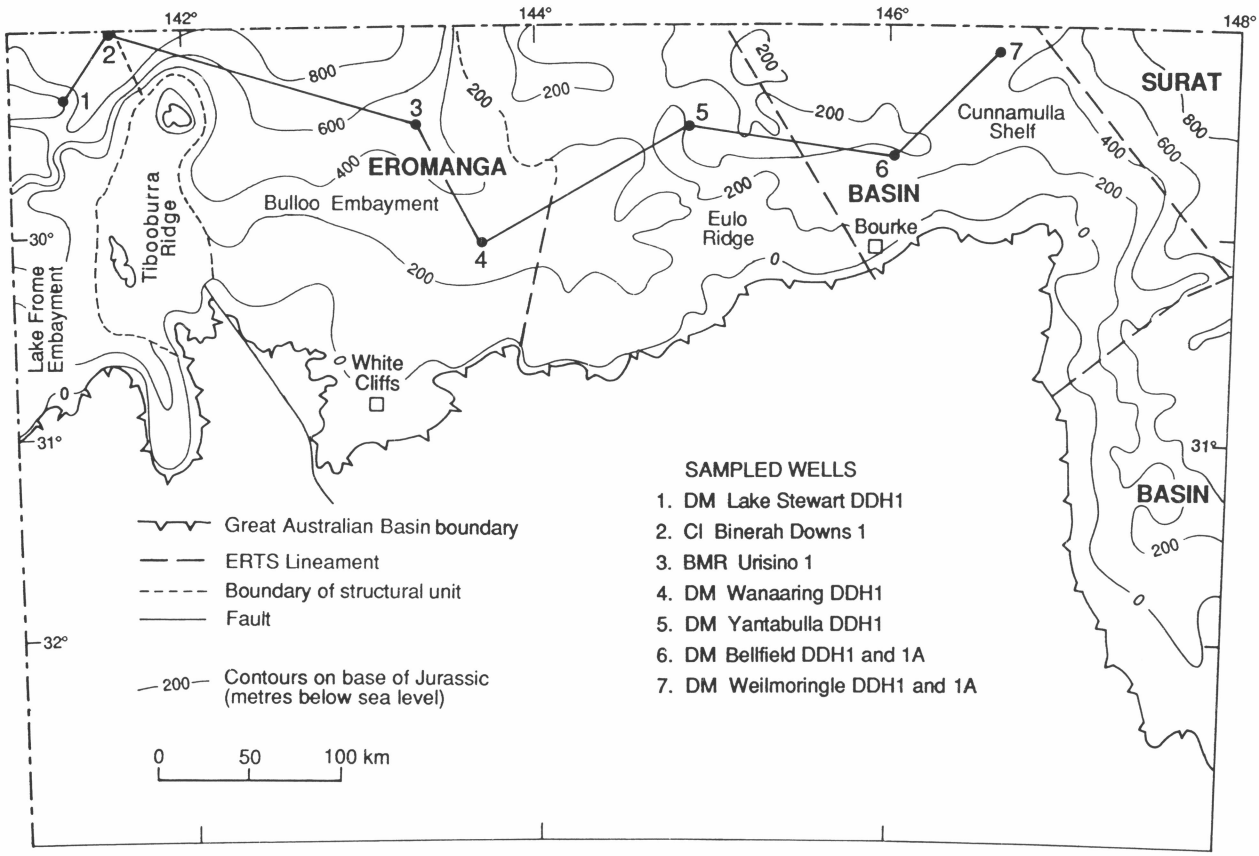

Figure 2. Structural elements of the Eromanga Basin in NSW and locations of sampled wells (1–7) along west–east transect. Structure contours (in metres below sea-level) on the base of the Jurassic System approximate isopachs of the Mesozoic basin-fill (after Cramsie & Hawke, 1984, their fig. 1.3).

talline quartz grains of vein and metamorphic origin are locally important in the quartzose petrofacies. Although many monocrystalline quartz grains in the volcanolithic sandstones are probably of volcanic origin, only rarely do they preserve unequivocal petrographic evidence of such affinity.

Feldspars comprise 20.0% and 3.1% (means) in the volcanolithic and quartzose sandstones, respectively (Table 2). In the volcanolithic sandstones, the feldspars have an average of 78.7% plagioclase and 21.3% K-feldspars (He, 1992, table 2.3, p. 47), the plagioclase being mostly andesine and oligoclase, and the alkali feldspars mainly sanidine and anorthoclase. In the quartzose sandstones, the plagioclase content averages 58.2% and the alkali feldspars 41.8% (He, 1992, table 2.3).

The quartzose sandstones have an average of 6.9% rock-fragments (RFGs) (Table 2), these being predominantly phyllitic and schistose grain-types, with subordinate grains of quartzose siltstone and sandstone and silicious VRFs (Table 3, Fig. 4B). The volcanolithic sandstones contain an average of 45.0% RFGs (Table 2), comprising mainly grains of andesite, phyllite and schist, and grains of quartzose siltstone and sandstone (Table 3, Fig. 4B). The VRFs in the volcanolithic sandstones are characterized by microgranular, lathwork, spherulitic and vitric textures; chloritized VRFs and grains of massive (i.e. non-schistose) chlorite are also common.

Mica, including degraded varieties of muscovite and biotite, averages 15.5% in the lithic sandstones, and 6.9% in the quartzose sandstones. Heavy minerals (mainly opaque minerals and tourmaline) amount to 0.28% in the volcanolithic sandstones and 0.17% in the quartzose sandstones, respectively.

Compaction

Sandstones of the Eromanga Basin in NSW have shallow burial depth (generally less than 1 km; Fig. 2). Non-ductile detrital grains (e.g. quartz, feldspars) show mainly point-contact and long-contact relationships (terminology of Taylor, 1950), commonly with ubiquitous free-margins (terminology of Allen, 1962; see also Wolf & Chilingarian, 1976, table 3–xviii) and, especially in the quartzose sandstones, little sign of deformation (Figs 5A,G, 6A,B, 7A,B, 8A-H, 9A-D). Ductile grains (fine-grained RFGs, mica and glauconie, etc.) show varying degrees of plastic deformation as a function of burial depth. In the volcanolithic sandstones of the Wallumbilla and Cadna-owie Formations and especially in the phyllarenitic phases of the Hooray Sandstone (particularly in Weilmoringle 1A), extensive plastic deformation of ductile grains has locally produced abundant pseudomatrix (cf. Dickinson, 1970) that has drastically reduced intergranular porosity and precluded/minimised subsequent growth of authigenic phases. Chemical compaction manifested by grains with sutured contacts has not been observed.

Infiltration clay

Mechanically infiltrated (MI) clays (cf. Matlack et al., 1989; Moraes & De Ros, 1990) are present at different

Table 2. Proportions (in QFL% ± 1 standard deviation) and ranges (in QFL%) of major detrital grain-types in sandstones of the Eromanga Basin in NSW. N = number of samples.

Formation	*N*	*Q*	*F*	*L*
Wallumbilla*	37	29.2±12.2	22.3±7.0	48.5±10.9
		5.7–63.9	10.4–41.6	20.6–67.3
Cadna-owie*	45	39.5±21.5	17.5±8.3	42.0±17.8
		10.9–91.6	1.8–37.2	4.3–72.9
Hooray Sdst./	43	90.2±8.2	3.1±3.1	6.9±7.1
Mooga Fm.		66.4–99.5	0.0–18.4	0.0–30.5
* volcanolithic sdst. (Wallumbilla + Cadna-owie)				
	82	35.0	20.0	45.0

levels within the fluvial Hooray Sandstone, manifested most conspicuously in porous sandstones by clay cutans (anisopachous grain-coatings of tangentially accreted lamellae) and meniscus-like inter-grain bridges of aligned clay-platelets. These clay platelets are characterized by mixed grain-/crystal-size and irregular grain-/crystal-morphology (Figs 5A-G). In plane-polarized light such cutans are variously translucent and light pinkish-brown or semi-opaque murky-reddish-brown to black, the translucent variety being optically coherent in crossed-polarized light with grey to honey-brown interference colour. In some samples, the semi-opaque reddish-brown grain-coatings and pre-overgrowth dust-lines on detrital quartz are very thin (Figs 5G, 8H), appear to contain little clay, and are probably veneers mainly of iron-oxide formed by very early precipitation in the zone of ground-water fluctuation.

More rarely in the Hooray Sandstone, the MI clay totally occludes the pore-spaces in the rock as optically-coherent grain-coating cutans and associated interstitial massive/loose aggregates (He, 1992, fig. 3.6a,b; cf. Moraes & De Ros, 1990, fig. 5E) and in some places provides a preferential substrate for the subsequent growth of small spidery bodies of siderite (cf. Fig. 8G). This type of MI clay is semi-translucent in plane-polarized light with very light-brown, grey or yellow first-order interference colours in crossed-polarized light. SEM and XRD analyses of this latter variety of MI clay (He, 1992, fig. 3.6c,d; and appendix 3.2.7) shows that it consists of kaolinite and mica, possibly illite. SEM study of the thin pinkish-brown variety of MI clay in the meniscus-like bridges confirms the sporadic presence of pseudohexagonal kaolinite crys-

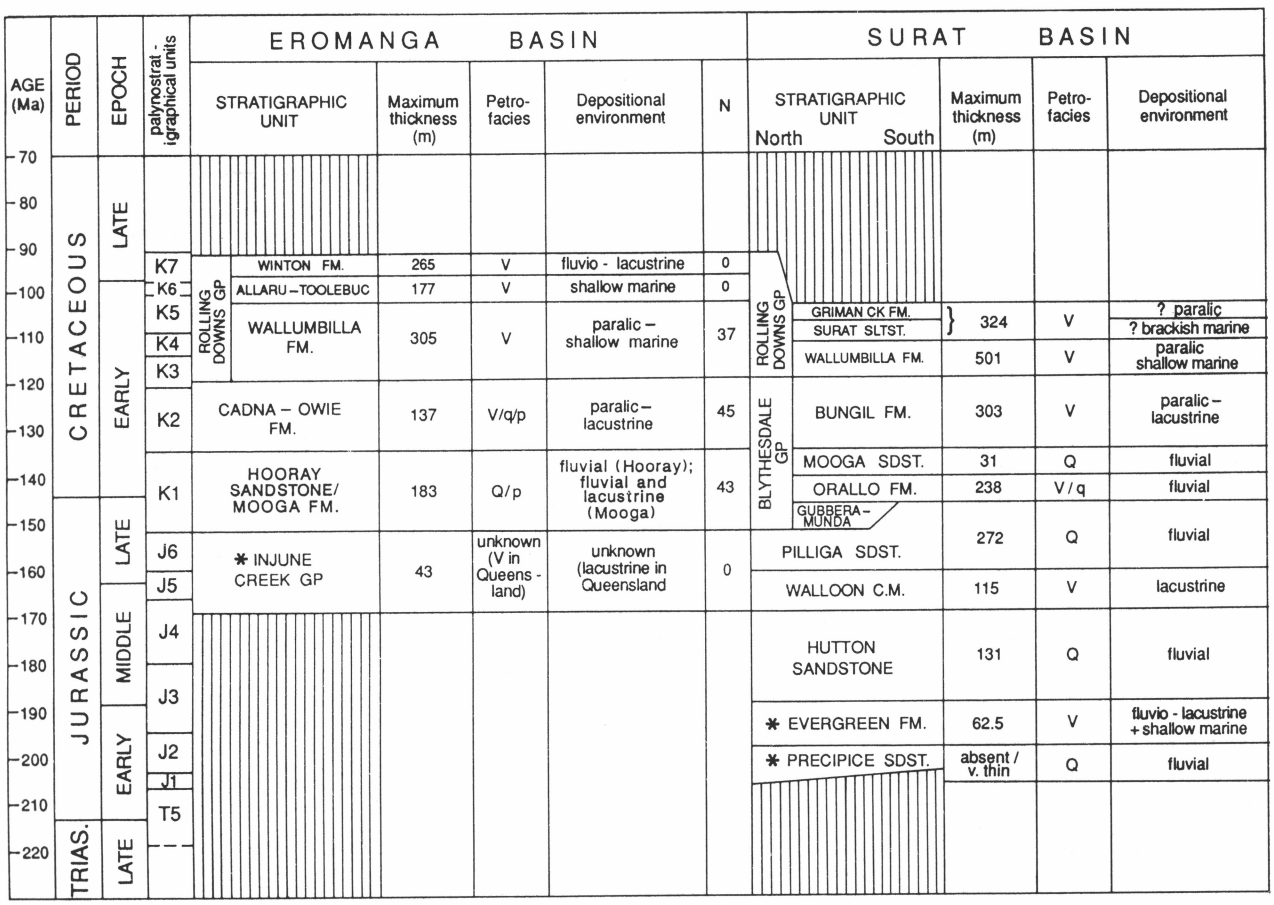

Figure 3. Details of the stratigraphy, depositional environments, thickness, and petrofacies characteristics of the Great Australian Basin succession in NSW compiled from various sources as follows.
Eromanga Basin: Hawke & Bourke (1984), Walsh (1985), Day et al. (1983), Etheridge et al. (1986), and He (1992). **Surat Basin:** Hawke & Bourke (1984), Bourke (1980), Geary & Short (1989), Exon (1976), and He (1992). Absolute geological time scale from Harland et al. (1982) and palynostratigraphical units and age control from Price et al. (1985). In the Eromanga Basin in NSW use of the term "Mooga Formation" follows Etheridge et al. (1986) and refers to the Hooray Sandstone equivalent in the Lake Frome Embayment where it comprises a lower fluvial Namur Sandstone Member and an upper lacustrine Murta Member. Jurassic succession of Surat Basin in NSW is similar to that of the Eromanga Basin in southern Queensland adjacent to the study area. Bold asterisks indicate formations that are thin and of limited development in the NSW part of the basin. Q = quartzose; V = volcanolithic; q/p = subordinate quartzose/phyllarenitic intervals; N = number of samples studied.

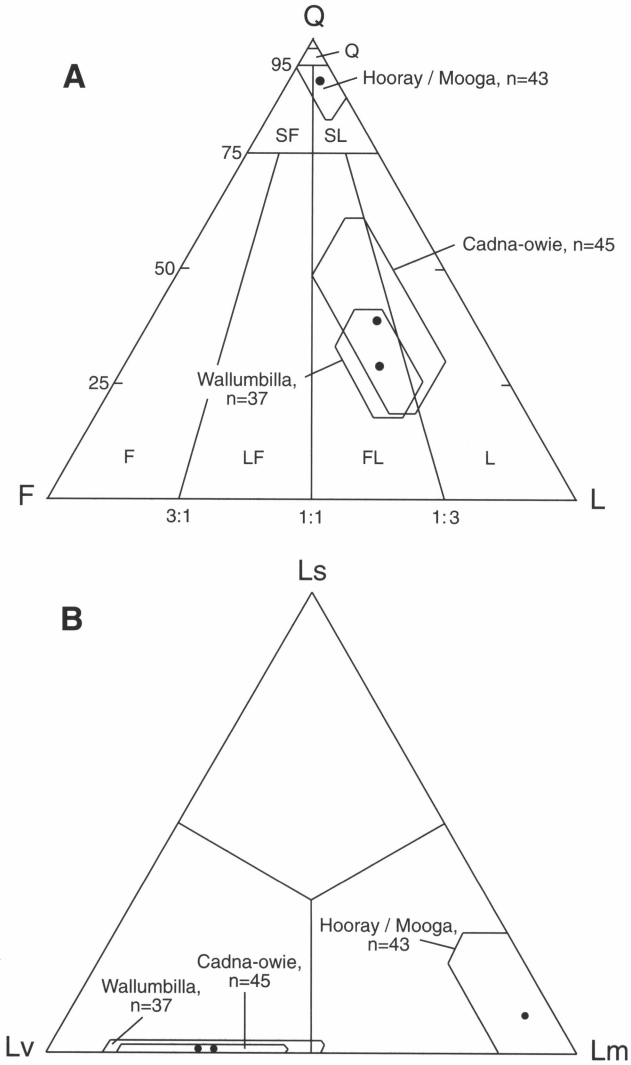

Figure 4. (A) Detrital modes (in QFL% ± 1 standard deviation) and (B) rock-fragment composition (in LvLsLm% ± 1 standard deviation) of sandstones of the Eromanga Basin in NSW.

tals (Fig. 5D) both as isolated platelets and as thin (1-to-3μm-thick) verms (i.e. stacked arrays or booklets). The crystal morphology of other clay particles present in these bridges is less diagnostic (Fig. 5E), but one crystal form present is like that of corrensite (chlorite/smectite; cf. Welton, 1984, p. 92-93). The orderly vermiform-like stacking of kaolinite crystals together with the interlocking web-like pattern of the corrensite-like mineral in the bridges suggests perhaps that these are *regenerated* mineral phases (in the terms of Wilson & Pittman, 1977) rather than manifesting textures that have arisen solely by mechanical lodgement.

Table 3. Proportions (in LvLsLm% ± 1 standard deviation) and ranges of rock-fragments (in LvLsLm%) in sandstones of the Eromanga Basin in NSW. N = number of samples.

Formation	*N*	*Lv*	*Ls*	*Lm*
Wallumbilla*	37	68.3±21.5	0.8±1.8	30.9±20.9
		26.0–97.2	0.0–9.5	2.9–72.8
Cadna-owie*	45	70.4±16.1	0.4±1.5	29.2±16.3
		0.0–97.9	0.0–9.4	2.1–98.8
Hooray Sdst./	43	5.2±9.2	8.2±18.1	86.5±20.7
Mooga Fm.		0.0–33.3	0.0–85.7	0.0–100.0
* volcanolithic sdst. (Wallumbilla + Cadna-owie)				
	82	69.4	0.6	30.0

Sporadic/rare quartz-overgrowths occur in some samples of the Hooray Sandstone that contain MI clay (Fig. 5F-H) present as thin cutans and inter-grain bridges, and are themselves either coated by these cutans or associated rims of iron-oxide (Fig. 5G), or appear to have grown penecontemporaneously with the accumulation of the MI clay (Fig. 5F,H). Matlock et al. (1989) and Moraes & De Ros (1990) argue cogently that MI clays form preferentially in coarser-grained sandy substrates characterized by lowered water-tables and episodic runoff with high concentrations of suspended-load clay that accumulates within the shallow subsurface; the meniscus-like bridges forming preferentially within the vadose zone, and the cutans and associated massive/loose aggregates forming preferentially within the more stagnant conditions of the phreatic zone or within perched water-tables. These circumstances are enhanced in coarse-grained fluvial environments characterized by an arid or semi-arid climate (Moraes & De Ros, 1990), circumstances that may have been met in large part during deposition of the Hooray Sandstone (cf. Slansky, 1984, p. 197–199).

Moraes & De Ros (1990) point out that, in general, "rocks with abundant infiltration clays show inhibited or aborted diagenetic evolution" because the clay cutans prevent or minimise quartz and feldspar overgrowth and inhibit calcite cementation, thus preserving much of the primary intergranular porosity (cf. Fig. 5A,G) though also reducing permeability to various degrees due to obstruction of the pore-throats (cf. Fig. 5B). These observations clearly also apply to those porous phases of the Hooray Sandstone that contain MI clay where sporadic/rare and mostly incipient quartz-overgrowths appear either to pre-date or to have grown penecontemporaneously with lodgement of the MI clay, but which clay largely terminated other diagenetic processes.

Minor proportions of clay (up to 20 whole-rock%) are also present as orthomatrix (cf. Dickinson, 1970) in some samples of the paralic and shallow-marine sandstones of the Cretaceous Cadna-owie and Wallumbilla Formations (He, 1992, appendix 3.3). Much of this clay has probably been introduced mechanically into the sand by bioturbation (cf. Byrnes, 1984, p. 130–131).

Grain dissolution and replacement

Dissolution and alteration of labile grains (i.e. feldspar, VRFs, and mica) are common and are especially important in the volcanolithic sandstones. Examples are the moldic or skeletal feldspars (Fig. 6A-C) and kaolinization of mica (Fig. 6H). These reactions release ions into the pore-fluid, thus contributing to the formation of authigenic minerals and secondary porosity. With the exception of sporadic kaolinite in some samples, the consistent absence of other grain-coating or pore-filling authigenic mineral phases within the intragranular pore-spaces of skeletal/moldic feldspars (e.g. Fig. 6A-C) suggests that the major phase of dissolution of the feldspar grains post-dates the growth of pore-filling or pore-lining authigenic cements other than kaolinite. This conclusion is also consistent with the observation that such delicate skeletal/moldic feldspars show little or no evidence of compactional deformation (Fig. 6A-C), suggesting that their

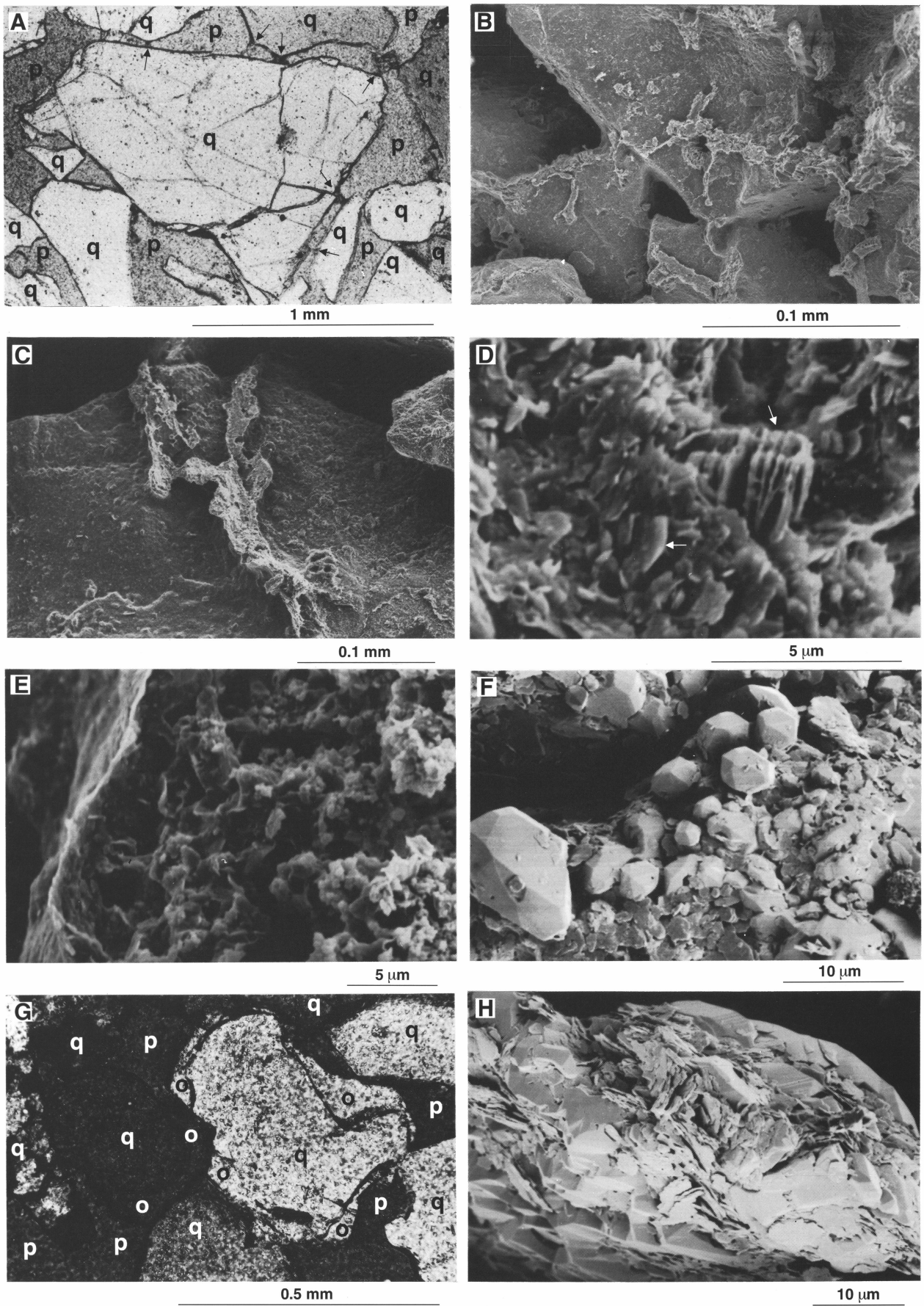
A
q
p
q
p
p
q
q
p
q
q
p
q
p
q
p
q
q
q
1 mm
B
0.1 mm
C
0.1 mm
D
5 μm
E
5 μm
F
10 μm
G
q
p
q
o
o
p
q
o
q
o
o
p
q
p
p
q
o
0.5 mm
H
10 μm

dissolution post-dated lithification of the host sediment. The partial to complete replacement by carbonate minerals of some labile grains, especially feldspar, is also sporadically common in the volcanolithic sandstones, and is an early diagenetic event, as will be argued below.

Authigenic minerals

On the basis of the petrographic evidence, the relative temporal order of appearance of the authigenic minerals in the volcanolithic sandstones is glauconie, pyrite, carbonates, smectite, zeolite, and kaolinite; and in the quartzose sandstones the order of appearance is quartz-overgrowth (phase I), chlorite, kaolinite and quartz-overgrowth (phase II).

Glauconie and pyrite

Authigenic mineral phases that stem from syndepositional to shallow-burial growth are glauconie/glauconite and iron-sulphide/pyrite. Byrnes (1984; and *in* Byrnes et al., 1975; and *in* Scheibnerová & Byrnes, 1977) describes glauconie as occurring in varying concentrations at different stratigraphic levels both within the Cadna-owie and the Wallumbilla Formations and relates its presence to times of slow sedimentation, which is consistent with modern concepts on the origin of the glaucony facies in Pliocene–Quatenary sediments (cf. Odin, 1988). The glauconie occurs predominantly as grey-green pellet-like grains which in particular beds in the Wallumbilla Formation attain proportions of as much as 15%-45% (Byrnes et al., 1975, p.3) and exhibit XRD characteristics (Byrnes et al., 1975, p.4) matched by those of ochreous-green glauconitized faecal pellets from modern environments (cf. Odin, 1988, p.233-236), suggesting that the authigenic phase of the pellets is an Fe- and K-rich smectite.

In the Wallumbilla Formation, authigenic framboidal pyrite is ubiquitous in addition to simple 0.5–2.0 mm spheroids lacking obvious substructure and macroscopic lumps of fine-grained pyrite (Byrnes, 1984, p.139). Additionally, our studies suggest that small isolated euhedral crystals of authigenic pyrite occur in the Wallumbilla Formation, and that such euhedral pyrite and pyrite framboids are also present in many samples of the Cadna-owie Formation. Some of the euhedral pyrite crystals have grain-coats of smectite, like that of neighbouring detrital grains, indicating their growth pre-dated that of the smectite cement. This authigenic pyrite manifests the precipitation of iron-sulphide within the anoxic–sulphidic environment in the shallow subsurface of organic-rich sediments deposited in marine/sulphate-rich environments (cf. Berner, 1981; Wolf & Chilingarian, 1988, 417–419; van der Weijden, 1992). Ferroan-carbonate-cemented hard-bands/concretions in both the Cadna-owie and Wallumbilla Formations contain authigenic pyrite framboids that pre-date the carbonate (cf. captions to Figs 8E,F, 9C), thereby demonstrating the temporal and spatial overprinting of anoxic–nonsulphidic-methanic diagenesis on that of the anoxic–sulphidic zone (cf. Berner, 1981, table 1, and p.364).

Carbonates

Carbonate cements are relatively rare to sporadic in the non-marine Jurassic part of the sandstone succession in NSW, but increase in relative abundance and mineralogical diversity in the lacustrine-to-paralic and shallow-marine Cretaceous strata where they are mainly confined to relatively thin zones or hard-bands and concretions (Tables 4,5).

Nodular siderite is the predominant carbonate in the Jurassic fluvial sandstones, and is present there in rocks with MI clay (Fig. 8G), suggesting that the siderite is of pedogenic origin. Both siderite and calcite occur in the hard-bands in the Cadna-owie and Wallumbilla Formations and in the Murta Member of the Mooga Formation (Figs 8E,F, 9A-C). Dolomite is very rare and is evident as single interstitial crystals or clusters of crystals in the Hooray Sandstone (Fig. 8H), and possibly also in the Cadna-owie Formation (Fig. 9B) where it is associated with complex siderite cement textures.

A more detailed account of these various carbonate cements and their stratigraphic context is given in Appendix 1,

Figure 5. Thin-section (A,G) and SEM photomicrographs (B–F, H) of MI clay fabrics and textures in the quartzose Hooray Sandstone.
(A) Coarse, porous and friable sandstone held together by very thin MI clay cutans (dark grain-coatings conspicuous along the free-margins of the grains) and inter-grain meniscus-like bridges (arrowed); plane-polarized light. q = quartz, p = pore. Weilmoringle 1A/25A, depth = 421.5 m, porosity = 33.50%, permeability = 4550.0 md. **(B)** Detail of same sample illustrated in A. Note the minor obstruction of pore throats by the coalescence of very thin MI clay cutans at grain contacts and the presence of meniscus-like bridges on grain surfaces elsewhere. **(C)** Detail of smooth-surfaced MI clay cutan and meniscus-like bridge in same SEM sample illustrated in B. **(D)** Interior of meniscus-like MI clay bridge illustrated in C. Note crude sub-alignment of clay platelets and what appear to be a single crystal and a verm of pseudohexgonal kaolinite (arrows). **(E)** Margin and adjacent interior of a meniscus-like MI clay bridge in the same SEM sample illustrated in B. Note (at left) smooth outer surface of the bridge, the irregular (?regenerated) texture of its interior, and the presence of curvilinear corrensite-like clay platelets at left just inside the margin. **(F)** Multiple syntaxial quartz-outgrowths on a detrital quartz grain coated by tiny platelets of MI clay. Note that some clay platelets also adhere to the crystal faces of some of the quartz-outgrowths, suggesting perhaps that the infiltration of the detrital clay and the development of the quartz-outgrowths were contemporaneous. The common syntaxial relationship of all crystal-outgrowths on a single parent quartz grain is indicated by the identical crystallographic orientation of each outgrowth as defined by the common alignment of like facets and their intersections. This holds both for the main field of outgrowths in foreground and for the background field at top-left. Wanaaring 1/11, depth = 388.9 m. **(G)** Thin-section photomicrograph (taken in partly crossed-polarized light) of a medium-grained quartzose sandstone showing sporadic small-scale overgrowths (o) on the free-margins of the detrital quartz (q) grains (at centre and at left); margins of overgrown detrital grains defined by dustline; p = pore. Murky-brown MI clay coats all grains, including the overgrowths themselves and also forms meniscus-like intergrain bridges in this sample (though the latter are not discernable in this photomicrograph). Textural relationships suggest that the overgrowths are not inherited and pre-date the MI clay cutans. Wanaaring 1/22, depth = 376.0 m. **(H)** Detrital quartz grain in sample of fine- to very-fine-grained sandstone containing MI clay and incipient quartz-outgrowths/overgrowths. Note the aligned fabric of the clay platelets, both tangential to the detrital grain surface in some places and orthogonal to the grain surface elsewhere in places where they lie adjacent to an individual quartz-outgrowth, perhaps suggesting progressive rotation of such clay platelet arrays concomitanly with the development of the quartz-outgrowth. Note too the irregular-shaped edges of the clay platelets which gives them an appearance similar to that of skeletal kaolinite and raises the possibility that the MI clay has been regenerated. Sample details as for F.

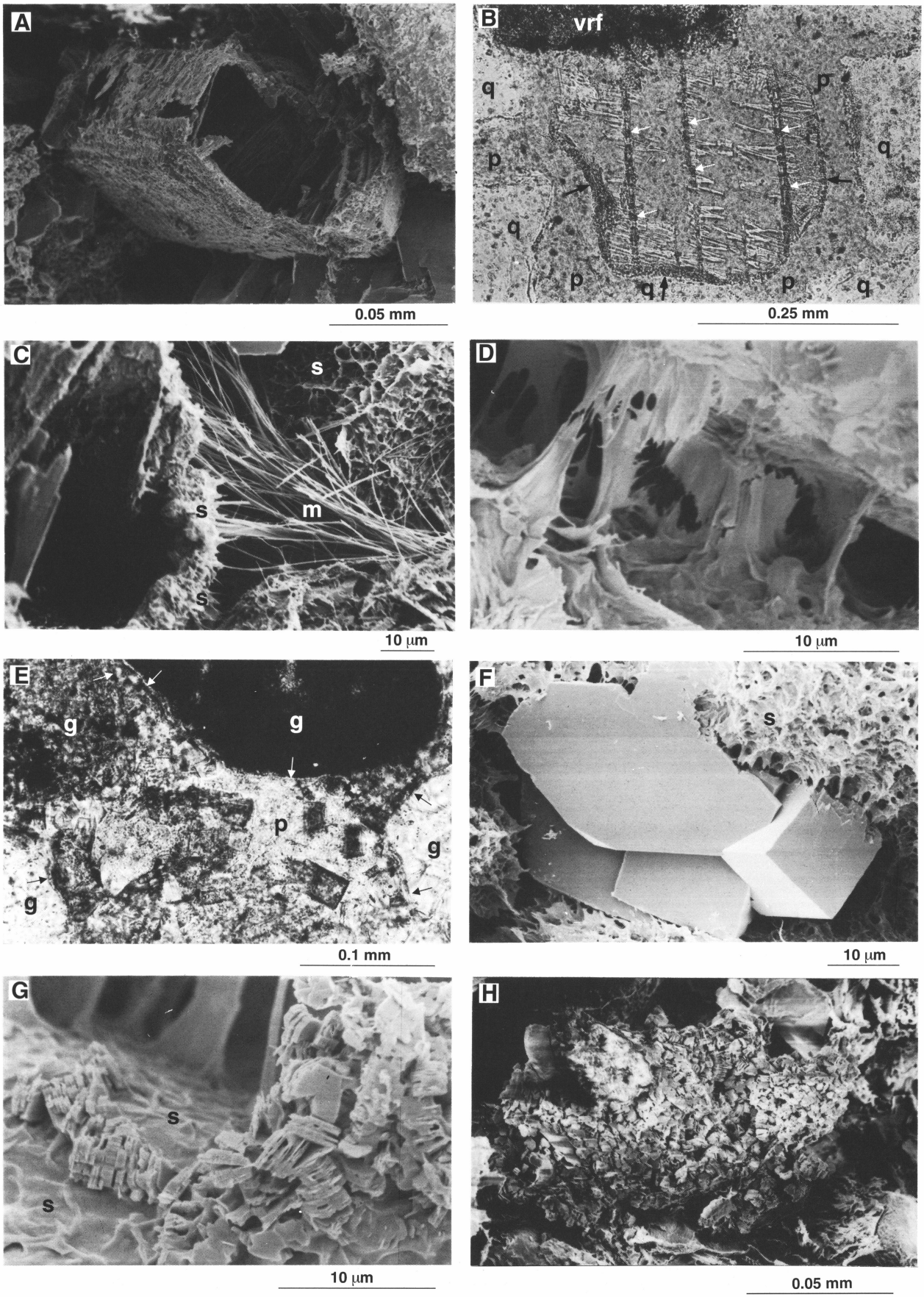
A
0.05 mm
B
vrf
q
p
q
p
q
p
q
p
q
0.25 mm
C
s
s
m
s
10 μm
D
10 μm
E
g
g
p
g
g
0.1 mm
F
s
10 μm
G
s
s
10 μm
H
0.05 mm

Table 4. Proportions of the main pore-filling diagenetic minerals (in whole-rock%) in sandstones of the Eromanga Basin, based on He (1992, appendix 3.3). Carbonate cements occur in only a few samples but tend to be predominant where present; "others" = mainly unidentified clay minerals. N = number of samples.

Formation	*Depth (m)*	*N*	*Authigenic type*	*Minerals range*	*Mean*
Wallumbilla		36	zeolite	0.0–27.4	3.20
			smectite	0.0–1.0	0.10
	50.0–		kaolinite	0.0–1.0	0.05
	321.6		carbonate	0.0–14.0	1.10
			others	0.0–19.8	3.40
Cadna-owie		45	kaolinite	0.0–4.4	0.60
			zeolite	0.0–2.0	0.08
	228.3–		smectite	0.0–1.4	0.07
	475.5		quartz	0.0–0.5	0.02
			carbonate	0.0–15.3	1.00
			others	0.0–29.2	4.00
Hooray Sdst./Mooga Fm.		43	quartz	0.0–1.6	0.10
	367.3–		kaolinite	0.0–0.8	0.07
	1098.3		carbonate	0.0–7.0	0.30
			others	0.0–34.1	6.50

where it is argued that most if not all of these cements are of early diagenetic origin, and that those in the paralic and shallow-marine strata are eogenetic products of methanic diagenesis (cf. Berner, 1981; Gautier & Claypool, 1984; van der Weijden, 1992).

The overall scarcity of carbonates in the Jurassic fluvial strata and their progressive upsequence increase in relative abundance and mineralogical diversity through the Lower Cretaceous lacustrine, paralic and shallow-marine succession (Table 5), appear to manifest the controlling influence of depositional environment and connate pore-fluids as well as organic-matter-content and sedimentation rate on carbonate authigenesis.

Smectite

Smectite clay cements amount to 0.1% on average in sandstones of the Wallumbilla Formation, and to 0.07% in those of the Cadna-owie Formation (Table 4). They comprise smectite, nontronite (Fe-rich smectite), and mixed-layer chlorite/smectite. Also, Slansky (1984, p.184 and fig. 6.5) reports accessory smectite in the Hooray Sandstone in Wanaaring 1 and Weilmoringle 1A.

Smectite occurs as grain-coatings in the form of irregular meshworks of wrinkled, wisp-shaped crystals (Fig. 6C,F,G), or as thin ribbons constituting pore-bridgings (Fig. 6G).

Nontronite occurs as crenulated blade-like pore-bridgings ranging in length and width up to about 10 μm (Fig. 6D); or as grain-coatings in the form of web-like crusts with a highly crenulated, fibrous morphology, with individual crystals orientated perpendicular to the detrital grain surfaces to which they are attached (He, 1992; appendix 3.1.7). Another type of nontronite grain-coating has a very fine-scaled asteriated morphology (He, 1992; appendix 3.1.6). The identification and differentiation of nontronite and ordinary smectite was confirmed by EDX spectra on the basis of their contrasting Fe content (He, 1992). Mixed-layer chlorite/smectite occurs as patchy grain-coatings and pore-fillings with a regular web-like morphology in the volcanolithic sandstones of the Wallumbilla Formation, the individual crystals coalescing to form regular reticulate networks.

The smectite clays are evidently among the earliest products of diagenesis in these rocks because they are commonly overlain by other authigenic minerals, including zeolites (Fig. 6C,E,F) and kaolinite (Fig. 6G).

Zeolite

Heulandite averages 3.2% in sandstones of the Wallumbilla Formation and 0.08% in those of the Cadna-owie Formation (Table 4). Mordenite (cf. Welton, 1984, p.128–129) was indentified in the Cadna-owie Formation of the Eromanga Basin in DM Weilmoringle 1A at 369 m depth of burial with approximate present formation temperature of 35°C (cf. Polak & Horsfall, 1979), a temperature that is perhaps indicative of the approximate thermal conditions under which the zeolite was precipitated (see also Byrnes et al., 1975, p.5). Both heulandite and mordenite overlie

Figure 6. Thin-section (B,E) and SEM (A,C,D,F–H) photomicrographs of altered labile grains and authigenic mineral phases in the quartzose/sublabile (A,B) and volcanogenic petrofacies (C–H).
(A) Moldic macropore in a skeletal feldspar grain caused by grain-dissolution. Cadna-owie Formation, Lake Stewart 1/4, depth = 695.2 m. **(B)** Skeletal feldspar grain coated by authigenic chlorite (dark outlines, arrowed in black, at left, bottom and right) which also thinly coats quartz (q) grains (at left and right) and forms tiny dark high-relief clots (arrowed in white) at regular intervals along prominent former ?cleavage and/or twin-planes that now survive as positive ribs within the moldic pore; vrf = volcanic rock-fragment, p = intergranular pore-space; plane-polarized light, sample details as for A. **(C)** Smectite (s) grain-coatings, mordenite (m) pore-bridgings and skeletal feldspar grain (at left) with moldic porosity. Cadna-owie Formation, Weilmoringle 1A/18, depth = 369.1 m. **(D)** Nontronite pore-bridgings, Wallumbilla Formation, Weilmorimgle 1/3, depth = 165.5 m. **(E)** Heulandite pore-fillings following very thin grain-coatings (arrowed) of smectite. The heulandite is the high-relief and/or dark-toned small rectangular crystals (at centre-bottom, -left and -right), the dark-toned crystals being ones that have taken up amaranth stain; p = pore, g = clastic grains; plane-polarized light. Wallumbilla Formation, Wanaaring 1/1, depth = 98.7 m, porosity = 39.9%, permeability = 25.0 md. **(F)** Smectite grain-coatings (s) and heulandite pore-fillings; Cadna-owie Formation, Weilmoringle 1A/18, depth = 369.1 m. **(G)** Smectite grain-coatings (s), pore-bridgings (top-centre), and skeletal kaolinite pore-fillings; Cadna-owie Formation, Lake Stewart 1/2, depth = 690.8 m. **(H)** Euhedral to subhedral kaolinite crystals replacing mica. Cadna-owie Formation, Wanaaring 1/4, depth = 310.3 m.

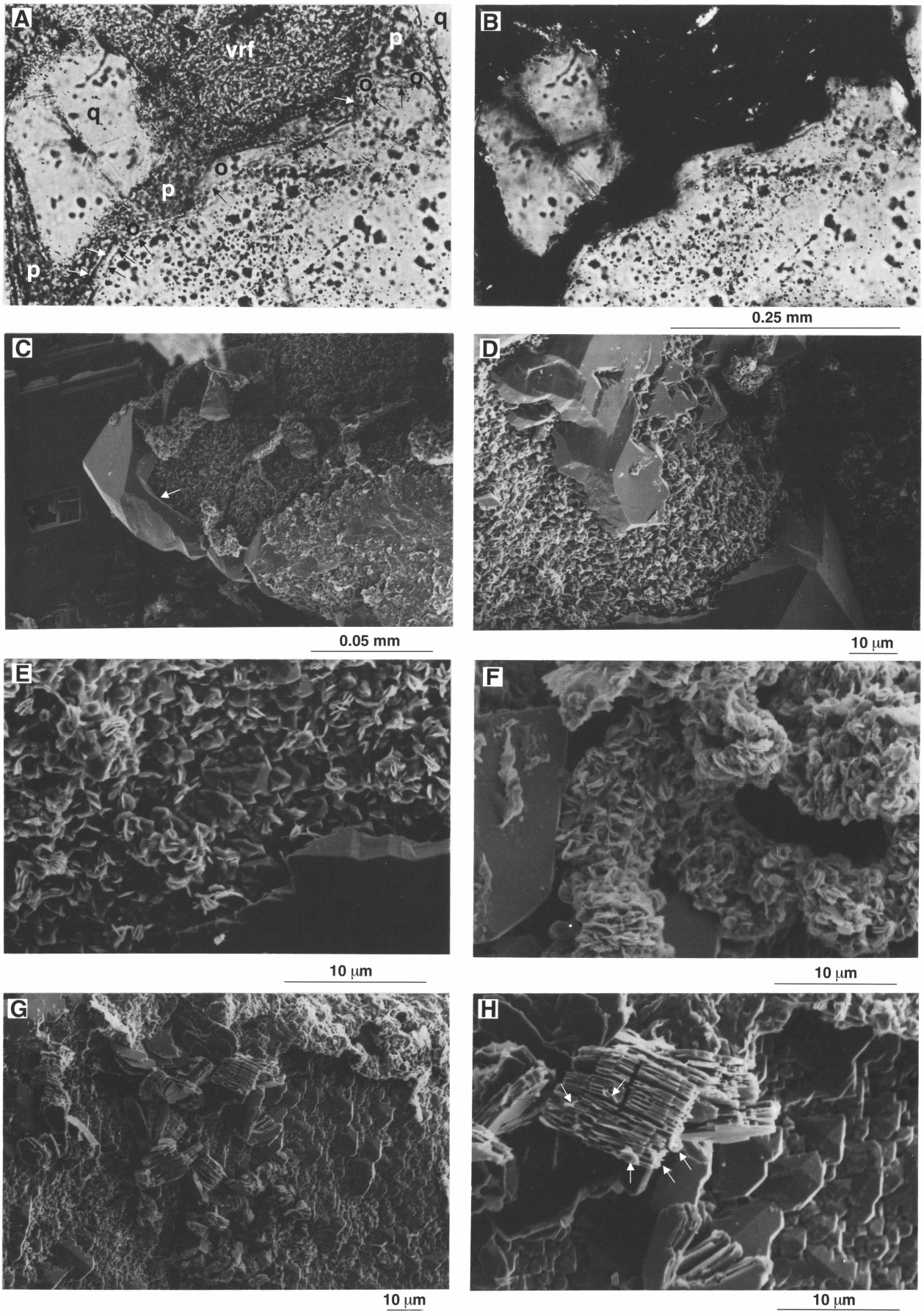
A
vrf
q
p
o
B
0.25 mm
C
0.05 mm
D
10 μm
E
10 μm
F
10 μm
G
10 μm
H
10 μm

the smectite grain-coatings in these rocks (Fig. 6C,E,F).

Heulandite has a blocky shape, a crystal size in the range of 10–40 μm, and occurs as pore-fillings, either as a large single crystal or as clusters of small crystals (Fig. 6E,F). Mordenite occurs as long curved rod-like fibres, a few tenths of a micro-metre in diameter, forming pore-bridges (Fig. 6C). Superficially, the morphology of mordenite is like the filamentous form of illite (cf. Welton, 1984, p.52–53): both have a hair-like appearance, but the mordenite fibres are characteristically more straight and larger in diameter. Mordenite coexists with smectite grain-coatings and partially dissolved labile grains (feldspar and VRFs) (Fig. 6C). EDX spectra of both heulandite and mordenite show that Si and Al are present as major constituents, and Fe and Ca as minor constituents (He, 1992, fig. 3.9c,d, and appendix 3.1.5a,b).

SEM photomicrographs of some samples show the heulandite crystals to exhibit localized patches of what appear to be dissolution-etch marks; similar marks were also observed in the Wallumbilla Formation by Byrnes (*in* Byrnes et al., 1975, p.5) and attributed by him to leaching by groundwater.

Kaolinite

Kaolinite averages 0.05% in sandstones of the Wallumbilla Formation, 0.60% in the Cadna-owie Formation, and 0.07% in the Hooray Sandstone (Table 4). It occurs in the sandstones as sporadic to semi-pervasive intergranular pore-fillings and as a replacement of labile detrital grains (e.g. mica and feldspar; Fig. 6H). Individual crystals of the kaolinite pore-fillings have a delicate skeletal shape, and they occur in random clusters or more typically in the characteristic verms (Figs 6G, 7G,H). In contrast, the kaolinite replacements of detrital grains (Fig. 6H) occur as delicate aggregates of the same overall size as the replaced detrital grains, but in which the individual kaolinite crystals are subhedral and finer-grained than the skeletal interstitial pore-filling variety. This contrasting degree of crystallarity[1] and relative crystal size between the pore-filling skeletal variety and the grain-replacement variety may manifest contrasts in the distant-versus-local sources of the constructing material and the general immobility of pore-fluid in these sandstones because the grain-replacement variety appears to be restricted to the volcanolithic sandstones, where average permeability is much less than that of the quartzose sandstones (Table 6; see also Slansky, 1984, p. 187).

Textural and stratigraphic relationships of the skeletal kaolinite pore-fillings with other diagenetic mineral phases suggests, with perhaps rare exception, that the skeletal kaolinite formed later than other authigenic minerals in these rocks.

Quartz

Quartz cement occurs predominantly in the quartzose Hooray Sandstone/Mooga Formation and in the more quartzose phases of the Cadna-owie Formation, and averages 0.10% and 0.02%, respectively (Table 4). It occurs mainly as embryonic or otherwise relatively small-scale syntaxial outgrowths/overgrowths (Figs 5F-H, 7A-H, 8A-E). Indeed, a remarkable feature of the quartzose sandstones is the general absence of ubiquitous, thick quartz-overgrowth cement (Figs 5A, 8C; see also Byrnes, 1984, p.127 and p.139). In some samples, the quartz cement is intergrown variously with authigenic chlorite (Figs 7A-F, 8D) and with MI clay (Fig. 5F) or perhaps with what could be platelets of kaolinite regenerated from MI clay (Fig. 5H), suggesting that there was overlap in the timing of their respective authigenesis/accumulation. In other samples, contrastingly, the incipient-to-small-scale quartz-overgrowths appear wholly either to pre-date thin grain-coatings of authigenic chlorite (e.g. in Wanaaring 1) or wholly post-date such chlorite grain-coatings (e.g. in the Namur Sandstone Member of the Mooga Formation in Lake Stewart 1; Fig. 8C). Additionally, in some samples of the lacustrine Murta Member of the Mooga Formation in Lake Stewart 1, quartz-overgrowths are sporadically developed in the coarser-grained laminae and pre-date pervasive poikilotopic calcite cement that is preferentially developed in the same coarse-grained layers (Fig. 8A,B), a pattern also present in the Murta Member in the Dullingari Murta Oilfield in South Australia (Ambrose et al., 1982).

Although perhaps not yet well constrained, the above patterns of cement stratigraphy suggest that two separate phases of quartz-overgrowths developed in the quartzose sandstones. Phase I quartz-overgrowth sporadically affected both the fluvial and lacustrine quartzose sandstones and was coeval with the accumulation of MI clay in the former (Fig. 5F-H) and coeval with the growth of authigenic chlorite grain-coatings in the latter (Figs 7A-F, 8D). Phase II quartz-overgrowth sporadically affects the fluvial quartzose petrofacies and, where present, wholly post-dates the authigenic chlorite grain-coatings (Fig. 8C). In samples that lack a cement-stratigraphic datum to either

Figure 7. Thin-section (A,B) and SEM photomicrographs (C–H) of cement-stratigraphic relationships among authigenic minerals in a quartzose/sublabile phase of the Cadna-owie Formation in sample Lake Stewart 1/4, at 695.2 m depth.
(A,B) Plane-polarized (A) and crossed-polarized (B) light views of incipient overgrowths/outgrowths on a detrital quartz grain and very thin and apparently multiple authigenic chlorite grain-coatings that both define the pre-overgrowth detrital grain margin in some places (arrowed in black) and also coat the overgrowth surface in tiny patches elsewhere (arrowed in white). All other detrital grains (q = quartz, vrf = volcanic rock-fragment) are coated with authigenic chlorite; p = pore. **(C)** Overgrown feldspar (left) and partly overgrown quartz grain (centre) on which authigenic chlorite grain-coat (rough-textured surface at centre, top and top-right) has arrested overgrowth development except where it is absent. Note the attempted transgression over the chlorite grain-coat by a minature flange (arrowed) of the quartz-overgrowth and the transgression (at top-centre-left) of a finger-like growth of the chlorite over the surface of the quartz-overgrowth. **(D)** Syntaxial outgrowths/overgrowth on a detrital quartz grain restricted to small patches by the inhibiting effect of a chlorite grain-coat in the intervening areas. **(E)** Detail of the chlorite grain-coat at bottom-centre in D. Note the presence (at centre) of minature pyramidal quartz outgrowths within the chlorite grain-coat. **(F)** Surfaces of quartz-outgrowth/overgrowth partly buried by grain-coating and pore-bridging authigenic chlorite. Note the crudely defined crystal-rosette pattern in the chlorite. **(G)** Quartz grain with numerous minature syntaxial outgrowths overlain by small clusters of skeletal kaolinite verms (left half of photograph) and by grain-coat of authigenic chlorite (light-toned area at top and top-right). Note that at top the chlorite grain-coat appears to overlie the kaolinite verms. **(H)** Detail of kaolinite verms illustrated at top-centre in G. Note the sporadic tiny authigenic chlorite crystals (arrowed white platelets) on the prominent kaolinite verm at centre-left, including two minature crystal-rosettes at the bottom-right of the verm.

[1] We use the term "crystallarity" to mean "degree of perfection of ideal crystal form" as distinct from "crystallinity", which for most mineralogists has connotations of degree of perfection of atomic-lattice-ordering.

Table 5. Distribution and mineralogy of authigenic carbonates in sandstones of the Great Australian Basin succession in NSW.

Formation	*Carbonate mineral phase*	*Mode of occurrence*	*Illustration herein*	*Environmental context of host sediment*	*Stage of diagenesis*	*Data sources*
Wallumbilla Formation	Ferroan-calcite, calcite and ankerite	Concretions (up to 2 m diameter), and fibrous and massive subhorizontal hard-bands up to 0.7 m thick, but typically 10–15 cm thick, some with cone-in-cone structure (in which the crystal fibres are arranged orthogonally to bedding). Massive calcite hard-bands (i.e., those lacking cone-in-cone or fibrous crystal structure) have small-scale poikilotopic crystals, in some samples exhibiting a crude sub-vertical elongate fabric of thick crystals that are coarser-grained than those in the cone-in-cone bands. Carbonate replaces framework grains in places.		Shallow-marine — paralic	early	Byrnes (1984) and present study
	Siderite	Massive hard-bands comprising pervasive finely-crystalline siderite rhombs and dense clusters of rhombs. Replaces framework grains in places.			early	Byrnes (1984) and present study
Cadna-owie Formation	Calcite and ferroan-calcite	Hard-bands and small modular masses of both fibrous calcite (with cone-in-cone structure) and poikilotopic calcite. Replaces framework grains in some samples.	Fig. 9C	Paralic — lacustrine	early	Byrnes (1984), Etheridge et al. (1986), and present study
	Siderite	(1) Minor hard-bands (as for Wallumbilla Formation); (2) Sporadic very fine crystals and small clusters of crystals associated with the hard-bands of poikilotopic calcite; (3) Zones (?hard-bands) cemented by pore-filling spherically-rimmed stellate crystal clusters which, in the plane of the thin-section, are either asymmetric and attached to detrital framework grains or more-or-less symmetrical with only parts of the annular rim attached to adjoining detrital framework grains as well as to the rims of adjacent stellate crystal clusters.	Fig. 9A, B		(1) early (2) early (3) early	Byrnes (1984), Etheridge et al. (1986), and present study
	?Dolomite	Sporadic interstitial rhombs within the siderite-cemented zones of (3) above.	Fig. 9B		?early	Present study
Mooga Formation (Murta Member)	Calcite, ferroan-calcite and ankerite	Hard-bands of very coarsely crystalline blocky poikilotopic calcite with minor phases of ferroan-calcite around immediate margins of detrital framework grains; developed preferentially in coarser-grained beds and laminae. Ankerite forms pore-fills in the associated laminae/beds of siltstone.	Fig. 8A,B	Lacustrine	?early	Etheridge et al. (1986), and present study
	Siderite	Zones of abundant small clusters of tiny siderite rhombs; developed preferentially in fine- and very-fine-grained sandstone.			?early	Present study
Mooga Formation (Namur Sandstone Member)	Siderite	Mainly very sporadic siderite rhombs and tiny clusters of rhombs forming pore-fills in the finer-grained sandstones.		Fluvial	?early	Etheridge et al. (1986), and present study
Hooray Sandstone	Siderite	Very small spidery to larger pervasive modular bodies of granular to semi-poikilotopic crystals developed preferentially in fine/very-fine- to medium-grained sandstones containing varying amounts of MI clay.	Fig. 8G	Fluvial	early	Byrnes (1984) and present study
	?Dolomite	Rare, sporadic euhedral rhomb-shaped crystals occurring interstitially either as isolated entities or in small clusters; preferentially developed in porous medium/fine-grained sandstone whose detrital grains are coated with thin iron-oxide rims.	Fig. 8H		?early	This study

Table 6. Range and mean (in brackets) of thin-section porosity (%) and core porosity (%) and permeability (md) of sandstones of the Eromanga Basin in NSW. Data from He (1992, appendix 4.2). N = number of samples.

Formation	*Depth (m)*	*N*	*T/S por. (%)*	*Core por. (%)*	*Permeability (md)*
Wallumbilla*	50.0–321.6	26	0.0–14.8 (4.8)	26.7–39.9 (35.8)	1.8–4805.2 (100.0)
Cadna-owie*	228.3–745.5	34	0.5–18.3 (4.8)	23.9–39.6 (33.5)	7.1–4691.0 (151.0)
Hooray Sdst./Mooga Fm.	367.3–1098.3	34	0.0–21.6 (9.3)	16.3–34.2 (28.9)	1.3–18400.0 (676.1)
* Volcanolithic sdst. (Wallumbilla + Cadna-owie)					
	50.0–745.5	60	0.0–18.3 (4.8)	23.9–39.9 (34.5)	1.8–4805.2 (128.9)

separate the phase I/II quartz-overgrowths (such as the post-phase I iron-oxide rims/MI clay cutans, cf. Fig. 5F,G; or authigenic chlorite grain-coatings, cf. Fig. 7C,D,F) or to constrain the phase I identity of the quartz-overgrowths through early terminal burial by pervasive carbonate cement (cf. Fig. 8A,B), quartz-overgrowths present in the rock may manifest a continuum of both phase I and phase II that is undifferentiable by normal light- and SEM microscopy.

Quartz-overgrowths are rare in the volcanolithic sandstones of the Wallumbilla Formation and where present appear to have grown in remnant intergranular pore-space not fully occluded by antecedant pore-filling cement (Fig. 8E).

Chlorite

Thin ubiquitous to sporadically developed chlorite grain-coatings occur in some of the quartzose and sublabile sandstones, particularly in the western part (i.e. Lake Frome and Bulloo Embayments) of the Eromanga Basin in NSW (cf. Slansky, 1984, fig. 6.5), and especially within sublabile phases of the upper part of the Cadna-owie Formation in Lake Stewart 1 (i.e. within the Wyandra Sandstone Member; cf. Etheridge et al., 1986, fig. 3; note that all SEM documentation of authigenic chlorite herein is from this stratigraphic unit). Petrographic observations (Figs 7, 8C,D) suggest that growth of these chlorite grain-coatings was both antecedant to and coeval with the growth of the incipient quartz-overgrowths in these sandstones; and consequently, where present, they inhibited the development of quartz-overgrowths both at the scale of individual detrital quartz grains (Fig. 7A-E) and more generally throughout the rock (Fig. 8C,D).

In the Wyandra Sandstone Member of the Cadna-owie Formation, thin-to-moderately thick chlorite grain-coatings, variously, are intergrown with rare feldspar-overgrowths on detrital feldspar grains (Fig. 8D), and/or simply coat such grains (Fig. 6B), typically in situations where such overgrown and chlorite-coated detrital feldspars are now preserved only as skeletal grains. The observation that some chlorite grain-coatings are actually intergrown with the feldspar-overgrowths suggests that the growth of both of these phases was contemporaneous. The chlorite is invariably absent within the intragranular moldic pores of these skeletal grains (Figs 6A,B, 8D), suggesting that the dissolution of the feldspars post-dated the growth of the chlorite grain-coatings and the associated feldspar-overgrowths. Where chlorite grain-coatings and pore-bridges coexist with skeletal kaolinite pore-fillings, the general relationship between them, as seen in thin-sections, is that the kaolinite post-dates the chlorite. However, in the Wyandra Sandstone Member of the Cadna-owie Formation (in sample Lake Stewart 1/4) SEM evidence shows local burial of the skeletal kaolinite by the chlorite grain-coat (Fig. 7G) and associated nucleation of rare tiny chlorite crystals on kaolinite verms nearby to the chlorite grain-coat (Fig. 7H); in this case, either the chlorite completely post-dates the kaolinite (in which case the kaolinite is an early diagenetic product) or else there was a phase of recurrent growth of the chlorite after its initial main phase of precipitation and the subsequent (late-diagenetic) interstitial growth of the kaolinite. The early diagenetic option for the kaolinite (cf. Fig. 10) is consistent with the observations of Ambrose et al. (1982, p.100) that an early but minor phase of kaolinite pore-filling characterizes the underlying Murta Member of the Cadna-owie Formation in the nearby Dullingari Murta Oilfield of South Australia. In that area, the kaolinite post-dates minor quartz-overgrowths and pre-dates pervasive calcite cement.

Cement stratigraphy

Certain aspects of the diagenetic history of the volcanolithic and quartzose sandstones are similar (Fig. 10). Early-diagenetic parallels involved physical compaction, either sporadic clay infiltration (Hooray Sandstone, Figs 5, 8G,H) or admixture through bioturbation (Cadna-owie and Wallumbilla Formations), and sporadic minor growth of carbonate cements (Figs 8A,B,E-H, 9A-C). Late-diagenetic parallels involved the dissolution of feldspar (Fig. 6A,B) and the concomitant growth of skeletal kaolinite pore-fills (Fig. 6G). In most other respects, the diagenetic histories of the two petrofacies differ (Fig. 10), mainly as a consequence of their respective different bulk mineralogies, organic content, and contrasted depositional settings (Fig. 3).

In the volcanolithic sandstones not pervasively cemented by carbonate, early-diagenetic leaching of the abundant volcanic glass led to the ubiquitous growth of smectite grain-coatings (Table 7, equation 1; Figs 6C-G, 10), closely followed by the leaching of plagioclase and the concomitant precipitation of pore-filling zeolite (Table 7, equation 6; Figs 6C,E,F, 10). Sporadic to common skeletal kaolinite pore-fills in these rocks stratigraphically overlie the grain-coating smectite (Fig. 6G). This suggests that they post-date both the smectite and the zeolite but does not otherwise finely constrain the timing of their formation. The speculation (Fig. 10) that they are of late-diagenetic origin is made by analogy of the similar pore-filling skeletal kaolinite in the quartzose sandstones where the

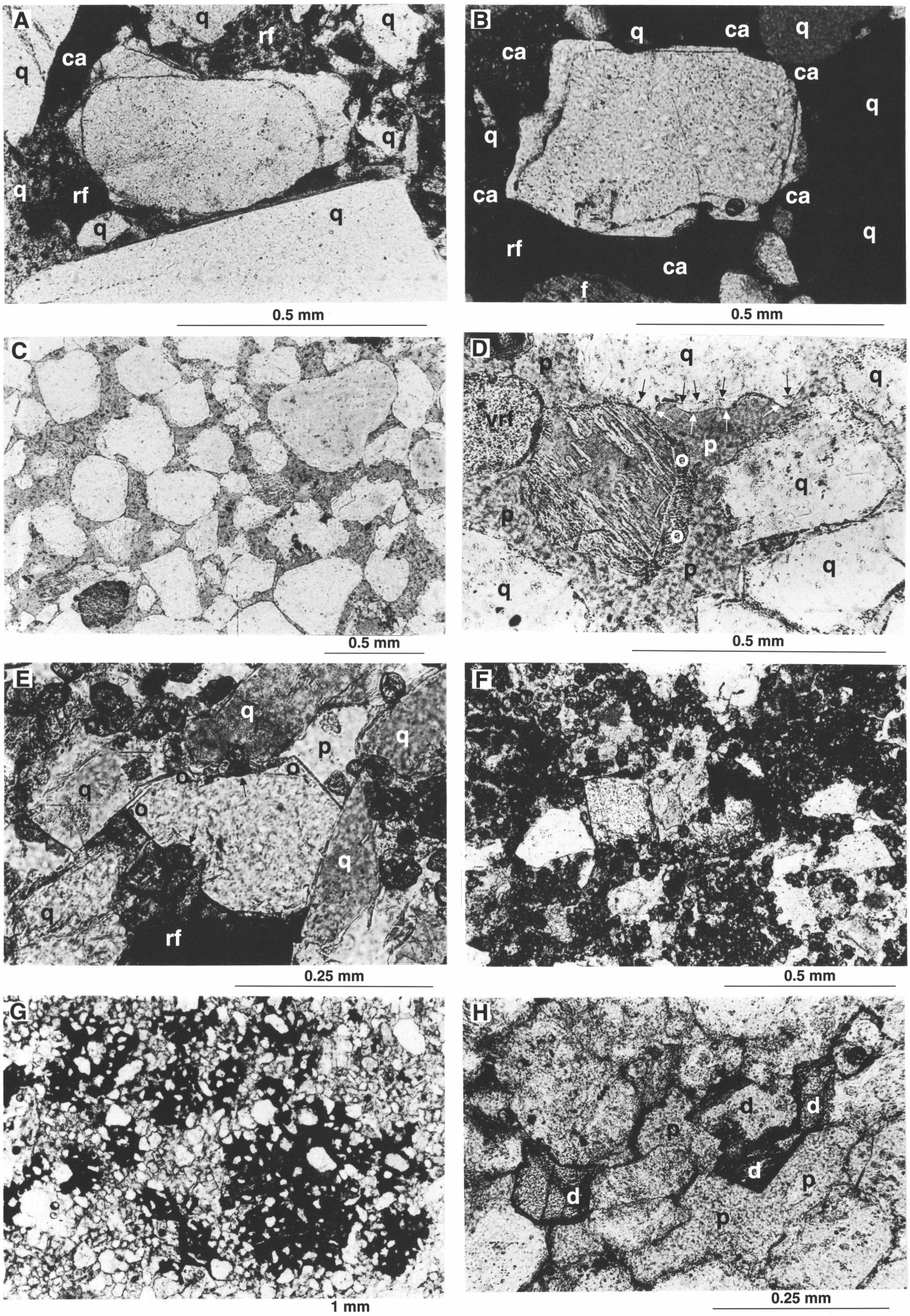
A
q
rf
q
ca
q
q
q
rf
q
q
0.5 mm
B
q
ca
q
ca
ca
q
q
ca
ca
q
rf
ca
f
0.5 mm
C
0.5 mm
D
p
q
q
vrf
p
o
q
p
o
p
q
q
0.5 mm
E
q
p
q
o
o
q
o
q
q
rf
0.25 mm
F
0.5 mm
G
1 mm
H
d
d
p
d
p
d
p
0.25 mm

timing of its growth is better constained (as discussed below).

Other diagenetic overprints evident in the volcanolithic sandstones include rare quartz-overgrowths that post-date carbonate cement (Fig. 8E), the kaolinization of mica (Fig. 6H), and the partial dissolution of feldspar. These overprints are interpreted to be of medial-to-late diagenetic origin (Fig. 10).

The quartzose sandstones show somewhat different patterns of diagenetic overprint in the eastern and western parts of the basin (i.e. in the Eulo Ridge– Cunnamulla Shelf and the Lake Frome Embayment, respectively; Fig. 2) with the intervening area (i.e. the Bulloo Embayment; Fig. 2) showing evidence of overlap of these two different patterns. These patterns manifest the influence on the preservation of intergranular porosity and on authigenesis caused, respectively, by: (1) the presence/absence of pedogenic overprint (i.e. iron-oxide rims and MI clay cutans); (2) the relative content of ductile detrital grains; and (3) the presence/absence of authigenic grain-coating chlorite.

In Wanaaring 1 (Bulloo Embayment) and in wells east thereof on the Cunnamulla Shelf (i.e. Bellfield 1A and Weilmorigle 1A; Fig. 2), the Hooray Sandstone shows evidence of pedogenic overprint (Figs 5, 8G,H) with associated preservation of primary intergranular porosity (Fig. 5A,G) except for local small-scale total occlusion of pores by pervasive MI clay and/or nodular siderite (Fig. 8G) and very minor partial occlusion by sporadic dolomite (Fig. 8H). Additionally, in Weilmoringle 1A, occlusion of primary pores on an even larger scale throughout much of the Hooray Sandstone stemmed from the early compaction of abundant phyllarenitic ductile grains into pseudomatrix which limited the infiltration of pedogenic clay and minimised the subsequent growth of authigenic phases. Incipient to small-scale quartz-overgrowths are present (Fig. 5F-H), some possibly antecedent to, or coeval with, the pedogenic clay. Additionally, authigenic chlorite of relatively early paragenetic origin is present in the Hooray Sandstone in Wanaaring 1 located in the Bulloo Embayment (but evidently not east thereof; see also Slansky, 1984), where it is sporadically associated with rocks containing MI clay and iron-oxide rims (Figs 5F-H, 8G,H), but evidently only as extremely thin grain-coatings. Apart from sporadic authigenic skeletal kaolinite pore-fillings, no other significant authigenic mineral phases occur in these sandstones east of the Lake Frome Embayment and they remain so weakly lithified that at some stratigraphic levels the rock "cannot be drawn up as core" (Byrnes, 1984, p.127).

In contrast, the quartzose sandstones of the Mooga and Cadna-owie Formations in the Lake Frome Embayment have few ductile grains, are evidently free of pedogenic clay, and are more effectively cemented (i.e. in Lake Stewart 1; note, however, that we have no sample control in the lowermost 37 m of the Mooga Formation in this well because of extensive core-loss over this interval). Incipient or small-scale quartz- and feldspar-overgrowths are the first authigenic phases, but whose continued development was variously arrested by chlorite grain-coatings (Figs 7A-G, 8C,D) or, within sporadic thin stratigraphic intervals, by pervasive poikilotopic calcite (Fig. 8A,B). Skeletal kaolinite is the only other significant authigenic non-carbonate phase in these quartzose sandstones and occurs as sporadic pore-fills both in intergranular and intragranular pores (Fig. 7G,H); and is generally more abundant in rocks with larger amounts of feldspar. The skeletal kaolinite sporadically occludes intragranular pores in skeletal feldspar suggesting that most of the kaolinite probably post-dates the feldspar dissolution, which in turn post-dates the feldspar-overgrowths and the authigenic chlorite (Figs 6B, 8D). How-

Figure 8. Thin-section photomicrographs of clastic textures and authigenic mineral relationships in sandstones of the quartzose/sublabile (A–D,G,H) and volcanolithic (E,F) petrofacies.
All photomicrographs are plane-polarized-light views except B which is taken in crossed-polarized light. **(A,B)** Coarse- to medium-grained quartzose sandstone cemented by very coarsely crystalline poikilotopic calcite (at extinction position in B) and subsidiary ferron-calcite with discontinous overgrowths on sporadic quartz grains (at centre in each photomicrograph). Textural relationships, including straight parallel edges of overgowth segments (as in B) and absence of overgrowth at points of contact between the host grain and neighbouring clastic grains (such as rock-fragment [rf] contacts in A; and quartz-grain contact at top-centre in B) indicate that the overgrowths are not inherited and therefore appear to pre-date the calcite cement. Calcite cement in A is dark-toned because of presence of carbonate-stain colours; q = detrital quartz, f = microcline feldspar, ca = calcite cement. Mooga Formation (Murta Member), Lake Stewart 1/9, depth = 768.7 m. **(C)** Abundant intergranular porosity (grey areas) and under-development of quartz-overgrowths in the Hooray Sandstone. The cement in this rock comprises very thin, discontinuous grain-coating authigenic chlorite followed by incipent, discontinuous quartz-overgrowths (present on most grains but not evident at this magnification), and rare kaolinite pore-fills and tiny clusters of siderite. Lake Stewart 1/15, depth = 811.1 m; detrital quartz = 73.6 whole-rock%; porosity 32.6%, permeability 9519.0 md. **(D)** Medium-grained quartzose/sublabile sandstone phase of the Cadna-owie Formation showing abundant primary intergranular porosity (p), secondary grain-dissolution porosity (at left) in skeletal feldspar, and sporadic thin quartz-overgrowths (arrowed in white) and ubiquitous thin authigenic chlorite grain-coats (dark grain outlines). Skeletal feldspar has a thin overgrowth zone (o) on its right margin intergrown (as demonstrated optically) with the authigenic chlorite grain-coat. Chlorite grain-coat defines detrital lower margin of quartz (q) grain (at top) evident as a discontinuous thin dark line (at tips of black arrows) beneath the overgrowth. vrf = volcanic rock-fragment. Lake Stewart 1/4, depth = 695.2 m (same rock as illustrated in Fig. 7), porosity = 31.5%, permeability = 4691.0 md. **(E,F)** Low (F) and higher (E) magnification views of fine-grained volcanolithic sandstone cemented predominantly by intergranular and grain-replacing siderite (small, dark-toned, high-relief grains), accessory intergranular heulandite and skeletal kaolinite (not discernable in photomicrographs) and rare quartz-overgrowth (o) (on grain at centre in E); p = pore, q = quartz, rf = rock-fragment. Note that in E, the termination of the quartz-overgrowth rims at places (arrowed) occupied by interstitial siderite suggests that the overgrowth post-dates the siderite. In F, note the dense clusters of siderite crystals in several places where they commonly replace labile clastic grains, especially VRFs, detrital chlorite and ?feldspar. In this rock, sporadic interstitial (non-replacive) siderite crystals contain pyrite framboids suggesting that the siderite post-dates the pyrite and therefore was precipitated in a non-sulphidic methanic environment. Wallumbilla Formation, Yantabulla 1/1, depth = 63.7 m, porosity = 31.5%, permeability = 567.0 md. **(G)** Very-fine-grained quartzose sandstone with MI clay (in light-toned intergranular areas) and pervasive nodular-shaped bodies of granular to finely poikilotopic siderite (dark-toned intergranular areas). MI clay is present throughout rock as cutans and massive aggregates and sporadically occludes the intergranular pores. Hooray Sandstone, Wanaaring 1/12, depth = 397.7 m, porosity = 22.2%, permeability = 13 md. **(H)** Medium- to fine-grained quartzose sandstone with thin brown iron-oxide-stained MI clay cutans (dark grain outlines) and sporadic euhedral rhombs of pore-filling ?dolomite (d), recognized by its clear-colour, strong rhombic habit, and rejection of carbonate-stain; p = pore. Hooray Sandstone, Wanaaring 1/11, depth = 388.9 m, porosity = 31.5%, permeability = 434.0 md.

ever, the minor stratigraphic overlap of authigenic chlorite on skeletal kaolinite (Fig. 7G,H) suggests that either some skeletal kaolinite pre-dates the chlorite or that the authigenic chlorite has continued to grow after a single major phase of kaolinite precipitation. Chemical considerations (discussed below) together with the textural evidence suggest that the major phase of feldspar dissolution was penecontemporaneous with the growth of the skeletal kaolinite and that both were late-diagenetic events (Fig. 10).

Regional correlation of authigenic mineral assemblages

As discussed in the above section, there is a noticeable change in the assemblage of authigenic minerals in the quartzose sandstones of the Eromanga Basin along the west–east transect. In the east, the authigenic phases are quartz-overgrowths and kaolinite in association with infiltration clay (possibly smectite, illite; cf. Slansky, 1984) or regenerated infiltration clay (kaolinite, ?chlorite/smectite; cf. Fig. 5D,E,H); in the western part of the basin, authigenic grain-coating chlorite occurs in association with quartz- and feldspar-overgrowths and kaolinite pore-fills.

X-ray powder-diffraction studies of the Eromanga Basin sediments in southern Queensland (Duff, 1987; Carmichael, 1989) revealed the authigenic mineral assemblage in the Hooray Sandstone to comprise quartz and kaolinite together with minor illite, illite/smectite and chlorite; and in the Cadna-owie Formation to be kaolinite and smectite

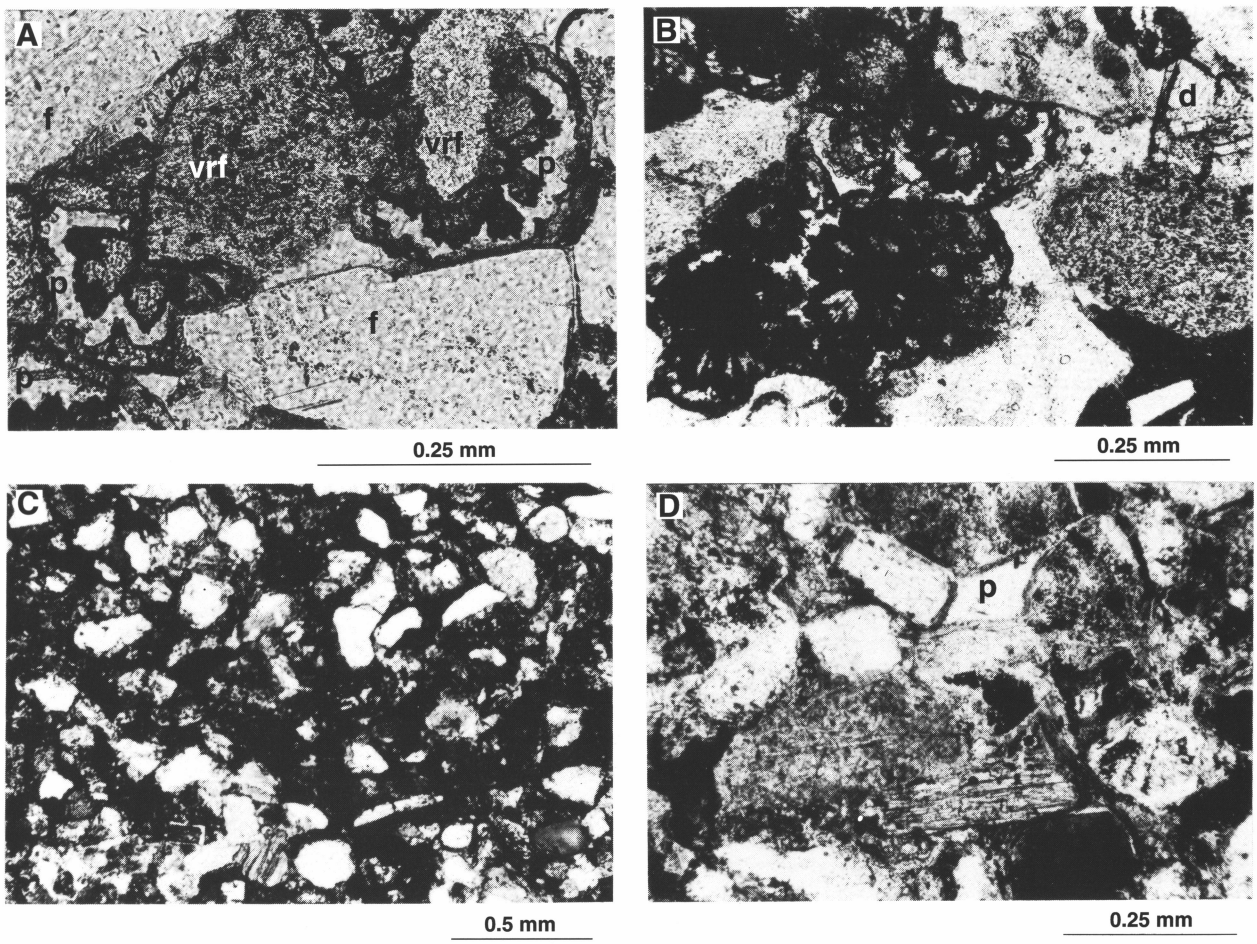

Figure 9. Thin-section photomicrographs, all taken in plane-polarized light, illustrating textures and authigenic mineral relationships in the volcanolithic sandstones.
(A,B) Medium-grained sandstone cemented by prominent pore-filling and grain-coating stellate clusters of rusty-brown siderite (dark-toned, high-relief radiating crystal arrays), each cluster being enclosed by a spherical/hemispherical siderite rim and intervening moat-like pore-space (p). In the two-dimensional thin-section view, the stellate arrays can be seen to be attached to and have grown outwards from the margins of clastic grains (as in A) or else appear to be unattached to and/or abut such grains and to radiate outwards from a centre located within the intergranular (former) void (as in B). Sporadic ?dolomite rhombs (d in B) are also present as intergranular cement; vrf = volcanic rock-fragment, f = plagioclase. Cadna-owie Formation, Weilmoringle 1A/40, depth = 342.7 m.**(C)** Fine-grained sandstone pervasively cemented by granular (not poikilotopic) calcite and minor ferroan-calcite (carbonate-stained dark intergranular areas). In some bedding-plane laminae within the same thin-section, the calcite is more coarsely crystalline, forming semi-poikilotopic crystals characterized by undulose extinction, and commonly replaces labile grains. Interstitial (non-replacive) calcite contains sporadic pyrite framboids suggesting that the calcite post-dates the pyrite and was precipitated in a non-sulphidic methanic environment. Cadna-owie Formation, Yantabulla 1/17, depth = 250.5 m, porosity = 5.0%, permeability = 1.0 md.**(D)** Fine-grained sandstone with sporadic isolated primary intergranular macropores (p), and pervasive grain-coating notronite cement that occludes most intergranular pores (evident as dark rims around some grains including those adjacent to the isolated macropore). Wallumbilla Formation, Bellfield 1A/24, depth = 206.3 m, porosity = 32.73%, permeability = 32.12 md.

with minor carbonate (siderite) and chlorite (Duff, 1987). In the South Australian and southwestern Queensland parts of the Eromanga Basin, the authigenic minerals in the lacustrine Murta Member of the Mooga Formation (equivalent of the upper part of the Hooray Sandstone) comprise the assemblage quartz–kaolinite–illite and locally carbonate (siderite, ankerite, and calcite) (Ambrose et al., 1982; Wall, 1987).

Similarly, in the neighbouring Surat Basin in Queensland Hawlader (1990a, fig.4; 1990b, fig.4) found the authigenic mineral assemblage in the equivalent quartzose phases of the Hooray Sandstone (i.e. the Gubberamunda and Mooga Sandstones; Fig. 3) to be quartz, chlorite, kaolinite, and minor carbonate and smectite; and in the Cadna-owie correlate (i.e. the Bungil Formation; Fig. 3) to be smectite, carbonate, and kaolinite. In the shallow-marine Rolling Downs Group Hawlader (1990b, fig. 4) found the authigenic mineral assemblage to be smectite, zeolite, carbonate, and kaolinite.

The remarkable similarities of the authigenic mineral assemblages across the southern Great Australian Basin are in keeping with the relatively uniform nature of isotopic compositions of the pore-fluids from these sandstones on a regional scale (Wall, 1987). This indicates insignificant isotopic exchange between pore-fluid and sandstone, notwithstanding the elevated temperature of the pore-fluid and the long distance and duration of its movement through the aquifer system of the basin (Wall, 1987).

Pore-types

Pores in sandstones may comprise primary and secondary macropores (i.e. pore-throat radius greater than 0.5 μm) and micropores (i.e. pore-throat radius less than 0.5 μm) (Pittman, 1979; Tingate & Luo, 1992). Macropores (whether primary or secondary in origin) consist of both intergranular and intragranular varieties (Table 1). Micropores comprise intragranular, intra-matrix, and intra-cement varieties.

Pore-types in the volcanolithic sandstones of the Eromanga Basin in NSW comprise micropores (Fig. 6C,D,F,G), grain-dissolution macropores (Fig. 6C) and isolated primary intergranular pores (Fig. 9D). Micropores are the dominant type in these rocks, and occur among the authigenic clay minerals (Fig. 6C,D,F,G) and degraded labile grains (feldspars, mica, and VRFs; Fig. 6C,H); macropores in these rocks are sporadically distributed and poorly interconnected (Figs 6C-H, 8E, 9A,B). Consequently, a representative sample of the volcanolithic sandstones from the Wallumbilla Formation (i.e. Bellfield 1A/24, Fig. 11A), which has 32.7% porosity and 32.1 md permeability, has more than 60% microporosity and less than 40% macroporosity.

Contrastingly, in the quartzose sandstones of the Eromanga Basin in NSW, the major pore-types comprise primary intergranular macropores (Figs 5A,B,G, 8C,D,H) and secondary grain-dissolution macropores (Figs 6A,B, 8D), both of which have good interconnections (Figs 5B, 8C). Consequently, a representative sample of the quartzose sandstones from the Cadna-owie Formation (i.e. Bellfield 1A/30, Fig. 11B), which has 31.2% porosity and 538.5 md permeability has nearly 70% macroporosity and about 30% microporosity. A more quartzose sample from the Hooray Sandstone (i.e. Bellfield 1A/31, Fig. 11C), which has 30.8% porosity and 269.7 md permeability, contains more than 80% macropores and less than 20% micropores.

Although there may be minor amounts of secondary intergranular pores in the Eromanga Basin sandstones in NSW as a consequence of dissolution of pore-fillings, particularly in the more porous quartzose sandstones that function as major aquifers (cf. Figs 5A, 8C,H), there is little compelling textural evidence for its existence. However, Ambrose et al. (1982) reported extensive intergranular cement-dissolution pores in the oil-productive Murta Member of the Mooga Formation in the Dullingari Murta Oilfield of South Australia, caused there by the dissolution of a formerly pervasive calcite cement prior to the entry of the hydrocarbons.

Porosity and permeability

In the volcanolithic sandstones, core porosity ranges from 23.9% to 39.9% (mean 34.5%); and permeability from 1.8 md to 4805.2 md (mean 128.9 md) (Table 6). In the quartzose sandstones, core porosity ranges from 16.3% to 34.2% (mean 28.9%); and permeability from 1.3 md to 18400.0 md (mean 676.1 md) (Table 6). These measurements can be expected to be overestimations, particularly in the case of the volcanolithic sandstones due firstly to their friable nature and high content of swelling (smectite) clay, and secondly to the artificial (i.e. laboratory) conditions under which the measurements were made relative to the natural subsurface conditions. Nevertheless, the resulting pattern in the porosity–permeability plot (Fig. 12) reflects a correlation between porosity/permeablity distributions and the depositional environments of these rocks (see also Table 8). The shallow-marine sandstones of the Wallumbilla Formation are volcanolithic, fine-grained and relatively well-sorted, and dominated mainly by smectite, zeolite, and kaolinite cements. The fluvial Hooray Sandstone and equivalent fluvial and lacustrine Mooga Formation are quartzose, fine to very coarse-grained and moderately sorted and have insignificant amounts of mainly quartz, kaolinite, and chlorite cements. Consequently, the quartzose sandstones have greater permeability with lower porosity in constrast to the volcanolithic sandstones (Fig. 12; Table 8). The lacustrine and paralic Cadna-owie Formation is an environmentally transitional unit between the Hooray Sandstone and the Wallumbilla Formation, and the petrological and petrophysical characteristics of its sandstones are more similar to the Wallumbilla Formation (Fig. 12).

Although characterized by similar values of porosity, the quartzose sandstones are more permeable than the volcanolithic sandstones (Fig. 12), and this reflects the influence of pore geometry on sandstone permeability. In comparison with the volcanolithic sandstones, the quartzose sandstones have more macropores that are well-connected by effective pore-throats of similar diameters, and that are characterized by larger ratios of pore-throat to pore-body size.

There is a weak trend suggesting that the porosity of the volcanolithic sandstones declines with increasing burial depth (Fig. 13A); but the porosity of the quartzose sandstones and the permeability of all sandstones show no trends with increasing burial depth (Fig. 13A,B; Table 6).

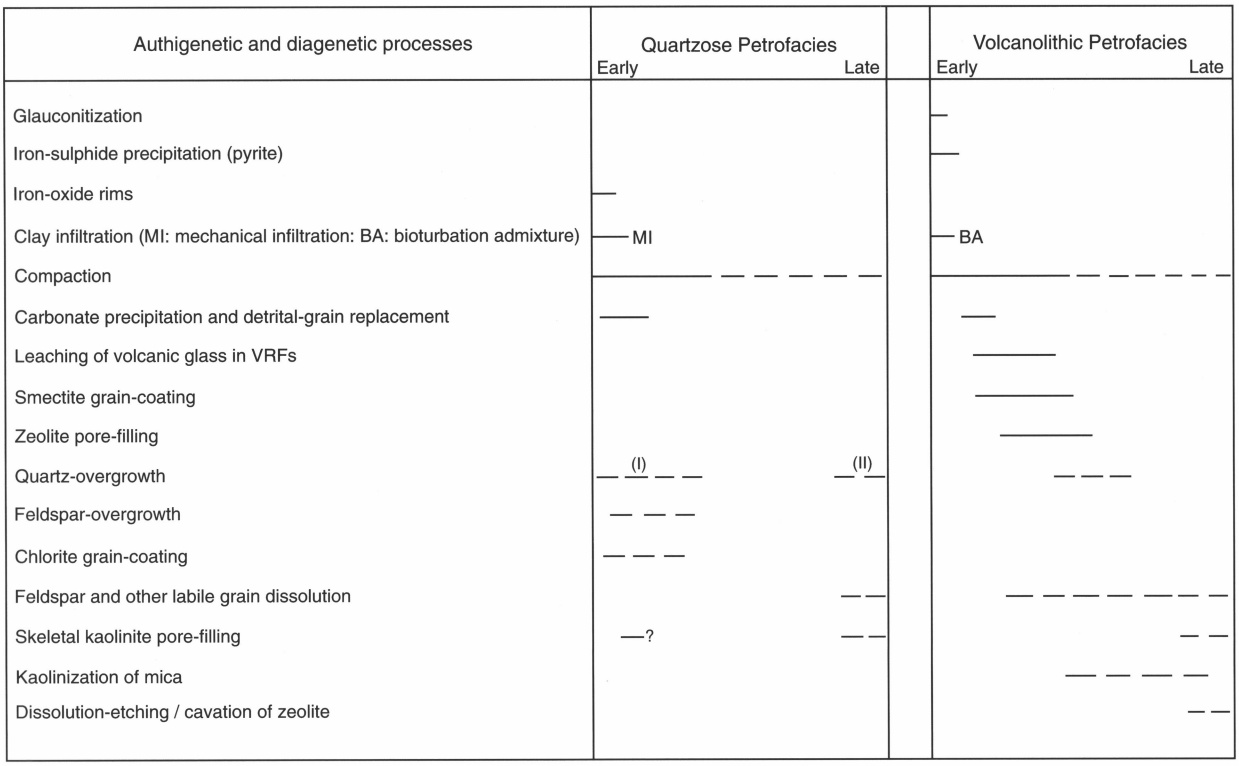

Figure 10. Paragenetic sequence of diagenetic/authigenic phases in the volcanolithic and quartzose sandstones of the Eromanga Basin in NSW.

Diagenetic mechanisms

Sandstones of the Eromanga Basin in NSW have shallow burial depths (in general <1 km). The present-day geothermal gradient in the study area varies geographically from 36° to 73°C/km, being greatest in parts of the Bulloo and Lake Frome Embayments, and predominantly in the range 40°– 60°C/km elsewhere (Hind & Helby, 1969, fig. 7.2A; Pitt, 1986, fig.7). The corresponding maximum formation temperatures are believed to be around 40°C. In the basinal succession in northwestern NSW, a vitrinite reflectance of 0.5% was recorded near the top of the Cadna-owie Formation in Binerah Downs 1 (Etheridge et al., 1986), indicating marginal thermal maturity.

In the volcanolithic sandstones, particularly within the shallow-marine Wallumbilla Formation, framboidal and macroscopic-nodular pyrites are common (Byrnes, 1984, p.139) as are the hard-bands and concretions of ferroan-calcite and siderite (Appendix 1); and evidently separately manifest early diagenetic precipitates within or related to the successively deeper microbial depth-zones dominated, respectively, by sulphate-reduction and carbonate-reduction/methane-generation (cf. Berner, 1981; Gautier &

Table 7. Some chemical reactions that have likely taken place in the Eromanga Basin sandstones (equations from Bjørlykke et al., 1979; McBride, 1987; Pettijohn et al., 1987; Vavra, 1989).

1.	$[Na_2KCaAl_5Si_{11}O_{32} + MgSiO_3] + H_2O + 4H^+ + 4HCO_3^-$ (Volcanic glass)	$\rightarrow Na(Al_5Mg)Si_{12}O_{30}(OH)_6 + Na^+ + K^+ + Ca^{+2} + 4HCO_3^-$ (Smectite)
2.	$2KAlSi_3O_8 + 2H^+ + 2H_2O$ (K-feldspar)	$\leftrightarrow Al_2Si_2O_5(OH)_4 + 4SiO_2 + 2K^+$ (Kaolinite)
3.	$4(Na_{0.5}Ca_{0.5})Al_{1.5}Si_{2.5}O_8 + 3H_2O + 6H^+$ (Plagioclase)	$\rightarrow 3Al_2Si_2O_5(OH)_4 + 4SiO_2 + 2Na^+ + Ca^{+2}$ (Kaolinite)
4.	$2KAl_3Si_3O_{10}(OH)_2 + 2H^+ + 3H_2O$ (Muscovite)	$\rightarrow 3Al_2Si_2O_5(OH)_4 + 2K^+$ (Kaolinite)
5.	$2K(Mg,Fe)_3AlSi_3O_{10}(OH)_2 + H_2O + 14H^+$ (Biotite)	$\rightarrow Al_2Si_2O_5(OH)_4 + 4H_4SiO_4 + 2K^+ + 6(Mg^{+2}, Fe^{+2})$ (Kaolinite)
6.	$Na_{0.6}Ca_{0.4}Al_{1.4}Si_{2.6}O_8 + 4.4H_2O$ (Andesine)	$\rightarrow 0.3CaAl_2Si_7O_{18}6H_2O + 0.5H_4SiO_4 + 0.8Al^{+3} + 0.1Ca^{+2} + 0.6Na^+ + 3.2OH^-$ (Heulandite)

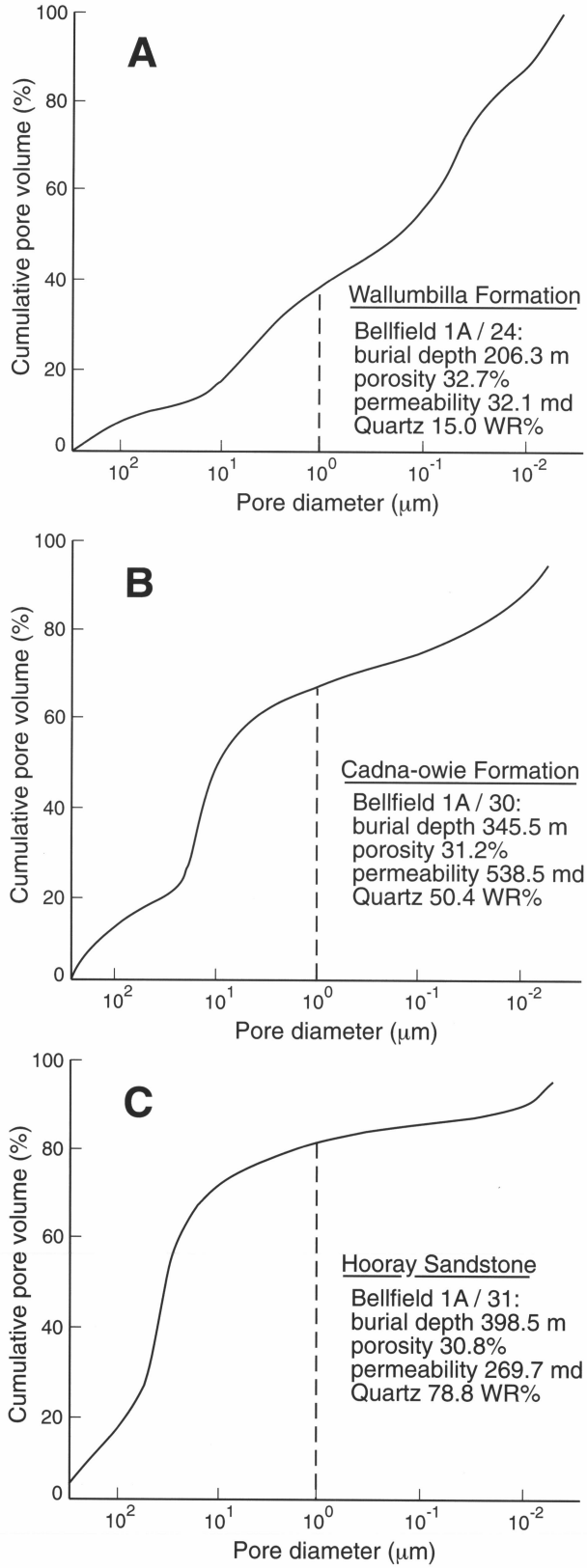

Figure 11A–C. Porosity distribution in representative sandstone samples of the Eromanga Basin in NSW illustrated by mercury injection curves.
A: microporosity comprises more than 60% of the total core porosity; **B:** macroporosity more than 60% of the total core porosity; **C:** macroporosity more than 80% of the total core porosity.

Claypool, 1984). Formation of these authigenic minerals suggests that the pore-fluid was alkaline and reducing (cf. Blatt et al., 1972, fig. 7.2; van der Weijden, 1992).

Subsequently, during early diagenesis of the volcanolithic sandstones, the leaching of labile grains (e.g. VRFs) by acidic pore-fluid led to the formation of smectite, and subsequently zeolite (resulting from increasing concentration of ionic species and pH) and kaolinite (Table 7). The likely source of acidic pore-fluid would have been the intercalated mudstones, which are rich in strongly biodegraded organic matter (Byrnes, 1984; Etheridge et al., 1986). Bacterial degradation of organic matter in organic-rich muds releases CO_2 and organic acids (McMahon & Chapelle, 1991; McMahon et al., 1992), which may enter the adjacent sandy sediments during compaction. Another source of acidic pore-fluid would have been related to thermal maturation processes at the later stage of diagenesis, which releases various organic acids (e.g. humic, amino, and carboxylic acids) (Schmidt & McDonald, 1979b; Tissot & Welte, 1984; Surdam et al., 1984) and these reagents may enter the intercalated sandstones during the diagenesis of the mudrocks. However, due to the marginal thermal maturity of the sediments of the Eromanga Basin in NSW, the organic acids released during thermal maturation of the organic matter would have played a limited role in the diagenesis of the volcanolithic sandstones. The volcanolithic sandstones and intercalated mudrocks have constituted an aquitard since the Plio-Pleistocene inception of the Great Artesian System (Habermehl, 1980, 1986), but this meteoric hydrological regime probably had only minor impact on the diagenesis of the volcanolithic sandstones.

The early diagenesis of the fluvial quartzose Hooray Sandstone in the eastern part of the basin was characterized by clay infiltration to form cutans that hindered the subsequent growth of authigenic phases except for localized precipitation of pedogenic siderite. In the fluvial and lacustrine sandstones of the Bulloo Embayment, the early development of incipient quartz-overgrowth (phase I, Fig. 10), which pre-date very thin chlorite grain-coats evidently resulted from the precipitation of silica from silica-enriched ground-water (mainly inherited from the fluvial and lacustrine environment) in which the silica-enrichment may have been due to the breakdown of labile grains. There is no evidence of pressure solution of detrital quartz grains, hence indigenous detrital quartz was not a source of the dissolved silica.

In the Lake Frome and Bulloo Embayments (i.e. in Lake Stewart 1 and Wanaaring 1), authigenic chlorite which variously either is coeval with or post-dates early quartz-overgrowths (phase I quartz-overgrowths, Fig. 10), or appears to wholly pre-date incipient quartz-overgrowths (phase II quartz-overgrowths, Fig. 10) is sporadically present in the fluvial and lacustrine quartzose Hooray Sandstone/Mooga Formation and in quartzose to sublabile lacustrine/paralic sandstones of the Cadna-owie Formation; the latter rocks, which have significant amounts of VRFs, feldspar and sporadic chamositic ooids, have more thickly developed authigenic chlorite which both pre-dates and is coeval with phase I quartz-overgrowths in the same rocks (Figs 7, 10). The formation of early authigenic chlorite in these sediments may have resulted from the alteration of ferromagnesian alumino-silicates, and iron-oxide and hydroxide (cf. Land & Dutton, 1978), which may have provided the necessary iron, aluminum and silica in reducing alkaline pore-fluids (cf. Iman & Shaw,

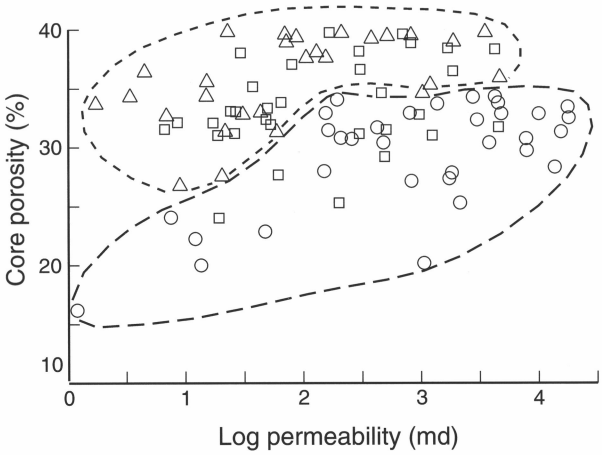

Figure 12. Relationship between core porosity (%) and log permeability (md) of the Eromanga Basin sandstones in NSW. Note that sandstones of the shallow-marine Wallumbilla Formation (triangles, n = 31) and those of the fluvial–lacustrine Hooray Sandstone/Mooga Formation (circles, n = 39) plot in separate fields, straddling which are the data points of the lacustrine–paralic Cadna-owie Formation (squares, n = 45).

1985). Syndepositional reducing conditions in the VRF-rich quartzose to sublabile sandstones of the Cadna-owie Formation are also indicated by the presence of the chamositic ooids (cf. Odin, 1988, p.28).

Since the Plio-Pleistocene, the quartzose Hooray Sandstone/Mooga Formation and the quartzose phase of the Cadna-owie Formation have functioned as major aquifers in the Great Artesian System (Habermehl, 1980, 1986). The artesian water is chemically of the sodium–bicarbonate–chlorite type and of meteoric origin (Habermehl, 1986), slightly acidic (e.g. H_2S and CO_2 are common gases in many water bores) and low in salinity (TDS range: 260–3917 mg/litre; Andrews, 1975), which favour the dissolution of feldspars and mica (equations 2–6, Table 7; Arditto, 1982, 1983; Garrels & Howard, 1957; Bjørlykke, 1981), and the formation of quartz and kaolinite cements. In addition, the circulating artesian water may be oversaturated with silica, thus providing a source of silica. This possibility is supported by the ubiquitous incipient quartz-overgrowths in the quartzose sandstones, some of which (i.e. phase II quartz-overgrowths) evidently post-date the authigenic chlorite (Fig. 8C). The equilibrium solubility of quartz in surface water is 6 ppm; and fluvial or surface water contains an average of 13 ppm dissolved silica, adequate to initiate precipitation of quartz (Blatt, 1979). Chemical analyses of artesian water from the Hooray Sandstone show the silica content to be around 20–30 ppm (Andrews, 1975). Considering that the equilibrium solubility of quartz at 50°C is about 21 ppm (Blatt, 1979), it is therefore possible that some of the latest (phase II) quartz cement may have precipitated from the artesian water. However, the overall scarcity of quartz cements in the quartzose sandstones (Figs 5A,G, 8C,D,H; Table 4) might in part reflect fluctuation of pore-fluid chemistry, partly due to the slow movement of the artesian water, estimated by Habermehl (1986) to be at a rate of about 1 m/day on the basis of hydrological data. Moreover, according to Bjørlykke & Egeberg (1993), at temperatures below 70°– 80°C, the rate of quartz precipitation from pore-fluid is very slow.

Table 8. Factors influencing the diagenesis of the volcanolithic and quartzose sandstones of the Eromanga Basin in NSW.

Petrofacies	*Volcanolithic*	*Quartzose*
Provenance	volcanic orogen	craton/recycled orogen
Chemical-reactivity	high	low
depositonal environment	lacustrine to shallow-marine	fluvial and lacustrine
texture	fine-grained well sorted	very coarse to fine-grained moderately sorted
Organic-content	high	very low (fluvial) and moderately high (lacustrine)
Pore-fluid	connate + fluid from mudrocks	connate + meteoric water
Compaction	moderate	slight to moderate
Diagenetic minerals	glauconie–pyrite–smectite–zeolite–kaolinite–carbonate	kaolinite–quartz–chlorite–carbonate
Porosity (%) (range/mean)	23.9–39.9/34.5	16.3–34.2/28.9
Permeability (md) (range/mean)	1.8–4805.2/128.9	1.3–18400.0/676.1

Cementation of the quartzose sandstones is more noticably developed in the western part (i.e. Lake Frome Embayment) of the Eromanga Basin in NSW, likely because:

- absence of abundant pseudomatrix, iron-oxide rims and MI clay that shield nucleation sites on detrital quartz and feldspar grains and prevent overgrowths (contrasting with the eastern part of the basin);
- although grain-coating authigenic chlorite is present in the sandstones, its development is sporadic and spatially discontinuous and has not wholly prevented overgrowth everywhere in the rock (cf. Figs 7A-D, 8C,D); and
- the southwestern region is closer to and includes part of the discharge area of the meteoric water (cf. Habermehl, 1986, fig.7); and the pore-fluid in the aquifer has a high concentration of dissolved ionic species.

This combination of circumstances contrasts with the eastern part of the basin which is adjacent to the recharge area of the meteoric water so that the material (e.g. silica) released from leaching of labile grains tends to be flushed away westwards more or less.

Conclusions

The diagenesis of the volcanolithic and quartzose sandstones of the Eromanga Basin in NSW manifests the influence of provenance and depositional environments on the compositions (e.g. detrital mineralogy and organic-matter-content) and the subsurface evolution of these rocks, as summarized in Table 8.

The diagenetic overprints comprise physical compaction, clay infiltration, dissolution and replacement of labile grains (feldspars, VRFs, and mica) and cementation by various mineral phases. In the lacustrine-to-paralic and shallow-marine volcanolithic sandstones of the Wallumbilla and Cadna-owie Formations, the authigenic mineral assemblage comprises syndepositional-glauconie, pyrite, smectite, zeolite, kaolinite, and sporadic carbonate; and the suite in the fluvial and lacustrine quartzose Hooray

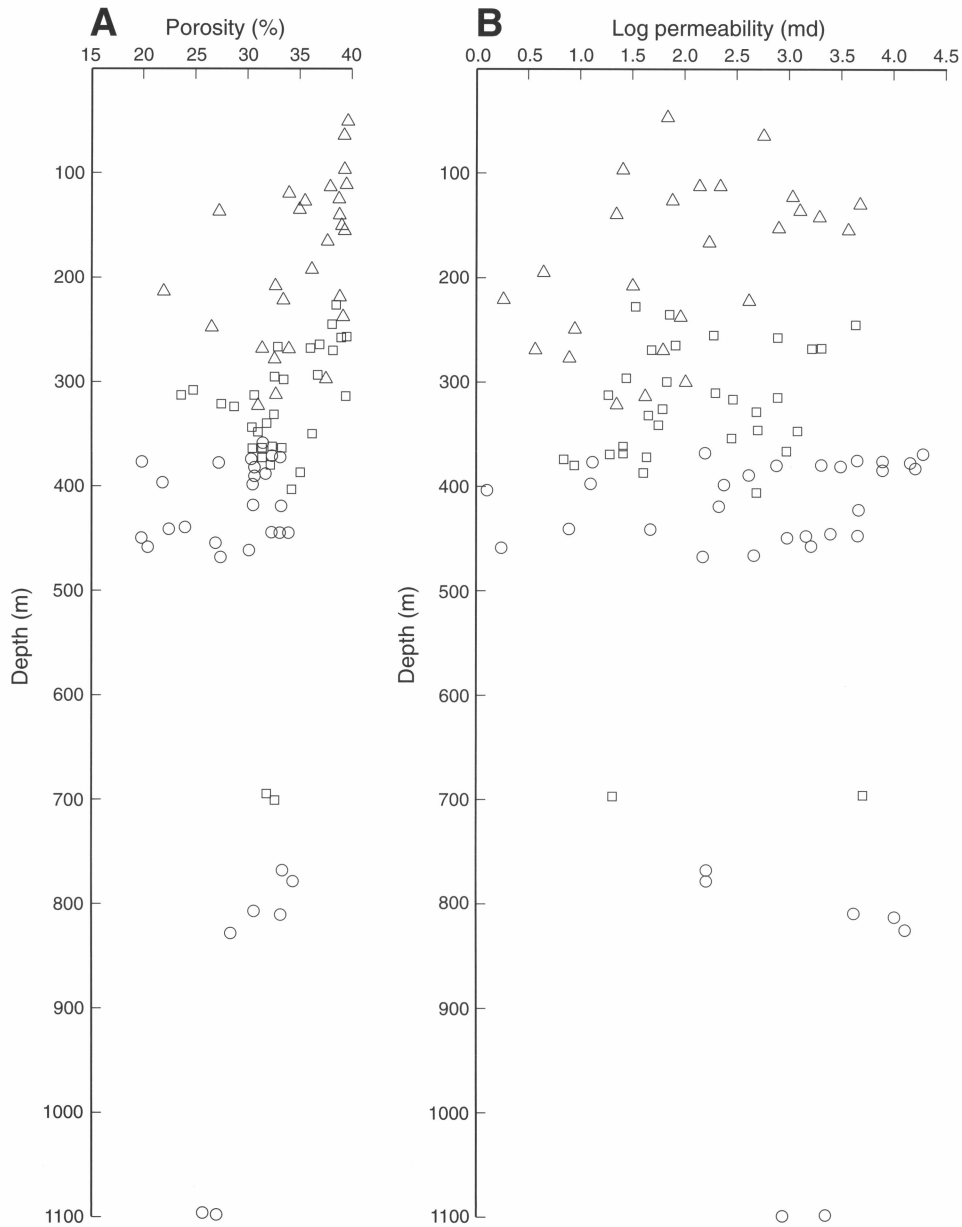

Figure 13. Scatter plots of sandstone core porosity (A) and log permeability (B) against burial depth. Data representations as in Figure 12.

Sandstone/Mooga Formation comprises quartz, kaolinite, and sporadic chlorite and carbonate. In the volcanolithic sandstones, micropores predominate. In the quartzose sandstones, the major pore-type is primary intergranular macropores, widely preserved by thin grain-coating cutans of pedogenic clay, and as a consequence these sandstones are relatively porous to highly porous and have good permeability. Accessory amounts of grain-dissolution macropores occur in rocks of both petrofacies, manifested in particular by skeletal and moldic feldspars. The development of secondary pores in the quartzose and volcanolithic sandstones is probably related to, respectively, the artesian water movement and the diagenesis of the intercalated organic-rich mudrocks.

Notwithstanding the very favourable porosity and permeability of, especially, the quartzose sandstones of the Eromanga Basin in NSW, these rocks are considered to have low reservoir potential primarily because of the absence of hydrocarbon source rocks and the absence of a regional seal.

Acknowledgements

We thank the Petroleum Resources Branch of the Bureau of Resource Sciences, Canberra, for permission to borrow core samples and Mr J. Staunton of their Core and Cuttings Laboratory, Canberra, for facilitating this loan; and Mr. S. Kaliza and staff of the Londonderry Core Library of the NSW Department of Mineral Resources for the loan of core samples, and Mr M. Hill of the NSW Department of Mineral Resources for the loan of thin-sections from DM Lake Stewart DDH1. We are grateful to the following persons for their generous accommodation of parts of the analytical work and their technical support: Associate Professor D. W. Emerson and Mr. P. Manning of the Department of Geology and Geophysics, the University of Sydney (petrophysical measurements); Dr J. Corcoran

of the Coal Technology Division, CSIRO, North Ryde (SEM-EDX analyses); Dr E. Slansky and Mr. A. Ferguson of the Geological Survey of NSW (XRD work); and Professor M. Wainwright of the Department of Chemical Engineering, the University of NSW (mercury intrusion porosimetry). We thank the following staff of Macquarie University for their technical assistance: Ms S. Doyle and Ms A. Gregor (SEM unit, School of Biological Sciences); Mr. Loc Van Duong and the late Mr R. Beaugeais (Petrographic Services, School of Earth Sciences); Mr K. Rousell (Cartographic Services, School of Earth Sciences). We thank Dr H. M. Hawlader for comments on an early draft of the paper and Drs J. Hamilton (CSIRO, North Ryde) and P.E. O'Brien (AGSO) for helpful reviews of the manuscript. Financial assistance was provided by the Ministry of Petroleum Industry of P. R. China, supplemented by grants-in-aid from the School of Earth Sciences of Macquarie University and private funding by the authors. We thank AGSO Corporate Publications staff for their professional input to the presentation of this paper, especially Dr K.H. Wolf (Senior Editor), and Ms Lana Murray and Mr Rex Bates (CSU).

References

Alder, D., 1993. Petroleum in New South Wales: an emerging opportunity. *In* Swarbrick, G. J. & Morton, D.J. (Editors). *NSW Petroleum Symposium, Proceedings*, June 1993. Petroleum Exploration Society of Australia, NSW Branch, 1–27.

Allen, J.R.L., 1962. Petrology, origin and deposition of the highest Lower Red Sandstone of Shropshire, England. *Journal of Sedimentary Petrology*, 32, 657–697.

Ambrose, G., Suttill, R. & Lavering, I., 1982. A review of the Early Cretaceous Murta Member in the southern Eromanga Basin. *In* Moore, P.S. & Mount, T.J. (compilers), *Eromanga Basin Symposium, summary papers*. Petroleum Exploration Society of Australia and Geological Society of Australia, 92–109.

Andrews, H.E., 1975. Artesian water quality in the New South Wales portion of the Great Australian Basin. *New South Wales Geological Survey Report* GS 1975/327 (unpublished).

Arditto, P.A., 1982. Deposition and diagenesis of the Jurassic Pilliga Sandstone in the southeastern Surat Basin, New South Wales. *Journal of the Geological Society of Australia,* 29, 191–203.

Arditto, P.A., 1983. Mineral–groundwater interactions and the formation of authigenic kaolinite within the southeastern intake beds of the Great Australian (Artesian) Basin, New South Wales, Australia. *Sedimentary Geology*, 35, 249–261.

Berner, R.A., 1981. A new geochemical classification of sedimentary environments. *Journal of Sedimentary Petrology*, 51, 359–365.

Bjørlykke, K., 1981. Diagenetic reactions in sandstones. *In* Parker A. & Sellwood B.W. (Editors). *Sediment Diagenesis*. D Reidel Publishing Company, Dordrecht, 169–213.

Bjørlykke, K. & Egeberg, P.K., 1993. Quartz cementation in sedimentary basins. *American Association of Petroleum Geologists Bulletin* 77, 1538–1548.

Bjørlykke, K., Elverhoi, A. & Malm, A.O., 1979. Diagenesis in Mesozoic sandstones from Spitsbergen and the North Sea — a comparison. *Geologische Rundschau,* 68, 1152–1171.

Blatt, H., 1979. Diagenetic processes in sandstones. *In* Scholle, P.A. & Schluger P.R. (Editors). Aspects of diagenesis. *Society of Economic Paleontologists and Mineralogists Special Publication* 26, 141–157.

Blatt, H., Middleton, G. & Murray, R., 1972. Origin of Sedimentary Rocks. *Prentice-Hall, Inc.* Englewood Cliffs, New Jersey, 634 pp.

Boone, G.M. & Wheeler, E.P., 1968. Staining for cordierite and feldspars in thin section. *American Mineralogist,* 53, 327–331.

Bourke, D.J., 1980. Stratigraphy of the Mesozoic sequence in the Warialda — Goondiwindi area. *Geological Survey of New South Wales Records* 19, 1–79.

Byrnes, J.G., 1984. Sedimentology of the Cretaceous marine sequence in the Eromanga Basin. *In* Hawke, J.M. & Cramsie, J.N. (Editors). Contributions to the Geology of the Great Australian Basin in New South Wales. *New South Wales Geological Survey Bulletin* 31, 125–142.

Byrnes, J., Morgan, R. & Scheibnerová, V., 1975. Recent evidence for the age of Great Australian Basin Cretaceous sediments in New South Wales. *Geological Survey of New South Wales Quarterly Notes,* 18, 2–13.

Carmichael, D.C., 1989. The Mineralogy of the Hooray Sandstone, Westbourne Formation, Birkhead Formation, Hutton Sandstone and the 'Basal Jurassic' unit in the southern Eromanga Basin, Queensland. *Queensland Department of Mines Record* 1989/7 (unpublished).

Cramsie, J.N. & Hawke, J.M., 1984. Introduction. *In* Hawke, J.M. & Cramsie, J.N. (Editors). Contributions to the Geology of the Great Australian Basin in New South Wales. *New South Wales Geological Survey Bulletin* 31, 1–22.

Day, R.W., Whitaker, W.G., Murray, C.G., Wilson, I.H. & Grimes, K.G., 1983. Queensland Geology, a companion volume to the 1:2,500,000 scale geological map (1975). *Geological Survey of Queensland Publication* 383, 194 pp.

Dickinson, W.R., 1970. Interpreting detrital modes of greywacke and arkose. *Journal of Sedimentary Petrology*, 40, 695–707.

Doutch, H.F. & Wilford, G.E., 1981. Sedimentary sequences. *In* BMR *Earth Science Atlas of Australia*. Bureau of Mineral Resources, Geology and Geophysics, Canberra.

Duff, P.G., 1987. The role of clays in formation damage in Mesozoic reservoir sandstones of the Eromanga Basin. *Bureau of Mineral Resources, Geology and Geophysics Record* 1987/14 (unpublished).

Etheridge, L.T., McMinn, A., Smyth, M., Walsh, I.L. & Davies, B., 1986. Eromanga Basin petroleum stratigraphic drill hole. *New South Wales Geological Survey Quarterly Notes*, 62, 16–30.

Exon, N.F.. 1976. Geology of the Surat Basin in Queensland. *Bureau of Mineral Resources, Geology and Geophysics, Bulletin* 166, 160 pp.

Folk, R.L., Andrews, P.B. & Lewis, D.W., 1970. Detrital sedimentary rock classification and nomenclature for use in New Zealand. *New Zealand Journal of Geology & Geophysics*, 13, 937–968.

Gallagher, K., 1990. Permian to Cretaceous subsidence history along the Eromanga-Brisbane Geoscience Transect. *In* Finlayson, D.M. (Editor). The Eromanga-Brisbane Geoscience Transect: a guide to basin development across Phanerozoic Australia in southern Queensland. *Bureau of Mineral Resources, Geology and Geophysics, Bulletin* 232, 133–142.

Garrels, R.M. & Howard, P., 1957. Reactions of feldspar and mica with water at low temperature and pressure. *Proceedings of the 6th Conference on Clay and Clay*

Minerals, 68–88.

Gautier, D.L., 1982. Siderite concretions: indicators of early diagenesis in the Gammon Shale (Cretaceous). *Journal of Sedimentary Petrology*, 52, 859–871.

Gautier, D.L. & Claypool, G.E., 1984. Interpretation of methanic diagenesis in ancient sediments by analogy with processes in modern diagenetic environments. *In* McDonald, D.A. & Surdam, R.C. (Editors). Clastic Diagenesis. *American Association of Petroleum Geologists Memoir* 37, 111–123.

Geary, G.C. & Short, D.A., 1989. Oil Company of Australia N.L. Chester-1 Well Completion Report PEL 182 New South Wales. *New South Wales Department of Mineral Resources Open-file Report* (WRC 233).

Green, P.M., Eadington, P.J., Hamilton, P.J. & Carmichael, D.C., 1989. Regional diagenesis — an important influence in porosity development and hydrocarbon accumulations within the Hutton Sandstone, Eromanga Basin. *In* O'Neil, B.J. (Editor). The Cooper and Eromanga Basins, Australia. *Proceedings of Petroleum Exploration Society of Australia, Society of Petroleum Engineers, Australian Society of Exploration Geophysicists (SA Branches)*, Adelaide, 619–627.

Habermehl, M.A., 1980. The Great Artesian Basin, Australia. *BMR Journal of Australian Geology and Geophysics,* 5, 9–38.

Habermehl, M.A., 1986. Regional groundwater movement, hydrochemistry and hydrocarbon migration in the Eromanga Basin. *Geological Society of Australia Special Publication* 12, 353–376.

Harland, W.B., Cox, A.V., Llewellyn, P.G., Picton, C.A.G., Smith, A.G. & Walters, R., 1982. *A Geologic Time Scale*. Cambridge University Press, Cambridge.

Hawke, J.M. & Bourke, D.J., 1984. Stratigraphy. *In* Hawke, J.M. & Cramsie, J.N. (Editors). Contribution to the geology of the Great Australian Basin in New South Wales. *Geological Survey of New South Wales Bulletin* 31, 23–115.

Hawlader, H.M., 1990a. Reservoir properties of some Surat Basin sandstones as a function of diagenetic clay-mineral assemblage. *Queensland Government Mining Journal,* 91, 180–189.

Hawlader, H.M., 1990b. Diagenesis and reservoir potential of volcanogenic sandstones — Cretaceous of the Surat Basin, Australia. *Sedimentary Geology,* 66, 181–195.

He, F., 1992. *Provenance, diagenesis and reservoir characteristics of sandstones of the Great Australian Basin succession in NSW*. Macquarie University, Sydney, PhD thesis (unpublished).

Hind, M.C. & Helby, R.J., 1969. The Great Australian Basin in New South Wales. *In* Packham, G.H. (Editor). The Geology of New South Wales. *Journal of the Geological Society of Australia*, 16, 481–497.

Imam, M.B. & Shaw, H.F., 1985. The diagenesis of Neogene clastic sediments from the Bengal Basin, Bangladesh. *Journal of Sedimentary Petrology,* 55, 665–671.

Jones, G.J. & Veevers, J.J., 1983. Mesozoic origins and antecedents of Australia's eastern highlands. *Journal of the Geological Society of Australia,* 30, 305–322.

Land, L.S. & Dutton, S.P., 1978. Cementation of a Pennsylvanian deltaic sandstone: isotopic data. *Journal of Sedimentary Petrology,* 48, 1167–1176.

Matlack, K.S., Houseknecht, D.W. & Applin, K.R., 1989. Emplacement of clay into sand by infiltration. *Journal of Sedimentary Petrology,* 59, 77–87.

McBride, E.F., 1987. Diagenesis of the Maxon Sandstone (Early Cretaceous), Marathon region, Texas: a diagenetic quartzarenite. *Journal of Sedimentary Petrology,* 57, 98–107.

McMahon, P.B. & Chapelle, F.H., 1991. Microbial production of organic acids in aquitard sediments and its role in aquifer geochemistry. *Nature,* 349, 233–235.

McMahon, P.B., Chapelle, F.H., Falls, W.F. & Bradley, P.M., 1992. Role of microbial processes in linking sandstone diagenesis with organic-rich clays. *Journal of Sedimentary Petrology*, 62, 1–10.

Moore, P.S., Hobday, D.K., Mai, H. & Sun, Z.C., 1986. Comparison of selected non-marine petroleum-bearing basins in Australia and China. *Australian Petroleum Exploration Association Journal,* 26, 285-309.

Moraes, M.A.S. & De Ros, L.F., 1990. Infiltration clays in fluvial Jurassic sandstones of Reconcavo Basin, Northeastern Brazil. *Journal of Sedimentrary Petrology,* 60, 809–819.

Odin, G.S. (Editor). 1988. *Green Marine Clays*. Developments in Sedimentology 45, Elsevier, Amsterdam, 445 pp.

Pettijohn, F.J., Potter, P.E. & Siever, R., 1987. *Sand and Sandstone* (2nd ed.). Springer-Verlag, Berlin, Heidelberg, 553 pp.

Pitt, G.M., 1986. Geothermal gradients, geothermal histories and the timing of thermal maturation in the Eromanga–Cooper Basins. *In* Gravestock, D.I., Moore, P.S. & Pitt, G.M. (Editors). Contributions to the geology and hydrocarbon potential of the Eromanga Basin. *Geological Society of Australia Special Publication* 12, 323–351.

Pittman, E.D., 1979. Porosity, diagenesis and productive capability of sandstone reservoirs. *In* Scholle, P.A. & Schluger P.R. (Editors). Aspects of Diagenesis. *Society of Economic Paleontologists and Mineralogists Special Publications* 26, 159–173.

Polak, E. J. & Horsfall, C. L., 1979. Geothermal gradients in the Great Australian Basin, Australia. *Bulletin of Australian Society of Exploration Geophysicists*, 10, 144–148.

Price, P.L., Filatoff, J., Williams, A.J., Pickering, S.A. & Wood, G.R., 1985. Late Palaeozoic and Mesozoic palynostratigraphical units. *CSR Oil and Gas Division, Palynology Facility, Report* 274/25 (unpublished).

Scheibnerová, V. & Byrnes, J.G., 1977. Correlation of Cretaceous lithostratigraphic, lithological, palynological, and foraminiferal units in the Great Australian Basin. *New South Wales Geological Survey Quarterly Notes,* 27, 1–11.

Schmidt, V. & McDonald, D.A., 1979a. Texture and recognition of secondary porosity in sandstone. *Society of Economic Paleontologists and Mineralogists Special Publication,* 26, 209–228.

Schmidt, V. & McDonald, D.A., 1979b. Secondary reservoir porosity in the course of sandstone diagenesis. *American Association of Petroleum Geologists Education Course Notes, Series* 12, 125 pp.

Slansky, E., 1984. Clay Mineralogy. *In* Hawke, J.M. & Cramsie, J.N. (Editors). Contributions to the geology of the Great Australian Basin in New South Wales. *Geological Survey of New South Wales Bulletin* 31, 179–214.

Surdam, R.C., Boese, S.W. & Crossey, L.J., 1984. The chemistry of secondary porosity. *In* McDonald, O. & Surdam, R. (Editors). Clastic Diagenesis.) *American Association of Petroleum Geologists Memoir* 37, 127–149.

Taylor, J.M., 1950. Pore space reduction in sandstones. *American Association of Petroleum Geologists Bulletin,* 34, 701–716.

Tingate, P.R. & Luo, P., 1992. Silica diagenesis and pore

development in the Permian sandstones, southern Cooper Basin. *Australian Petroleum Exploration Association Journal,* 32, 325–338.

Tissot, B.P. & Welte, D.H., 1984. *Petroleum Formation and Occurrence* (2nd ed.). Springer-Verlag, Berlin, 699 pp.

van der Weijden, C.H. 1992. Early diagenesis and marine pore water. In Wolf, K.H. & Chilingarian, G.V. (Editors). *Diagenesis, vol. III. Developments in Sedimentology* 47. Elsevier Scientific Publishing Company, Amsterdam, 13–134.

Vavra, C.L., 1989. Mineral reactions and controls on zeolite-facies alteration in sandstones of the central Transantarctic Mountains, Antarcticia. *Journal of Sedimetary Petrology*, 59, 688–703.

Walsh, I.L., 1985. Eromanga Basin NSW — petroleum data package. *New South Wales Geological Survey Report* GS 1985/007, 143 pp.

Wall, V.J., 1987. Hydrocarbon reservoir quality in the Cooper, Eromanga Basins. *Department of Earth Sciences, Monash University, National Energy Research, Development and Demonstration Program Report* 722 (unpublished).

Welton, J. E., 1984. *SEM Petrology Atlas*. American Association of Petroleum Geologists, Tulsa, 237 pp.

Wilson, M.D. & Pittman, E.D., 1977. Authigenic clays in sandstones: recognition and influence on reservoir properties and paleoenvironmental analysis. *Journal of Sedimentary Petrology*, 47, 3–31.

Wolf, K.H. & Chilingarian, G.V. 1976. Diagenesis of sandstones and compaction. *In* Chilingarian, G.V. & Wolf, K.H. (Editors). *Compaction of Coarse-Grained Sediments, vol. II. Developments in Sedimentology* 18B. Elsevier Scientific Publishing Company, Amsterdam, 69–473.

Wolf, K.H. & Chilingarian, G.V. 1988. Ore-related diagenesis — an encyclopedic review. *In* Chilingarian, G.V. & Wolf, K.H. (Editors). *Diagenesis, vol. I. Developments in Sedimentology* 41. Elsevier Scientific Publishing Company, Amsterdam, 25–553.

Appendix 1. Details of carbonate cements

Carbonate cements occur sporadically in both the volcanolithic and quartzose sandstones (Table 4). They are relatively rare in the non-marine Jurassic part of the succession (i.e. Hooray Sandstone and Namur Sandstone Member of the Mooga Formation), but become increasingly more frequent in bedding-parallel hard-bands and concretions in the Lower Cretaceous lacustrine, paralic, and shallow-marine units (i.e. Murta Member of Mooga Formation, Cadna-owie, and Wallumbilla Formations; Table 5).

Sporadic to rare siderite is the main carbonate mineral in the Jurassic fluvial strata and in the Hooray Sandstone occurs both as microscopic spidery/nodular and macroscopic nodular growths that preferentially frequent sandstones with MI clay (Fig. 8G). This intimate association of the nodular siderite with pedogenic clay suggests that this siderite is probably an early diagenetic (eogenetic) phase and formed under reducing conditions at or near the syndepositional water-table in sands whose permeability had been diminished through the uptake of MI clay through influent seepage. Rare larger crystals of pore-filling ?dolomite (recognized by its strongly euhedral rhombic habit, coarser grain-size, clear colour in plane-polarized light, and rejection of carbonate stain colour) also occur in the Hooray Sandstone in porous rocks with very thin MI ferruginous cutans or iron-oxide rims (Fig. 8H) and is possibly also a relatively early diagenetic phase, though there is no available textural evidence to constrain this speculation. Rare small interstitial crystal-clusters and isolated rhombs of siderite also occur sporadically in the fluvial Namur Sandstone Member of the Mooga Formation, particularly in the finer-grained rocks (Table 5). No calcite is evident in samples of the Jurassic fluvial sandstones (see also Byrnes, 1984, p.140; and Etheridge et al., 1986, fig.3).

Although still stratigraphically sporadic, a more varied assemblage of carbonate minerals and associated crystal textures are present in the overlying Lower Cretaceous lacustrine, paralic and shallow-marine strata (Table 5). Bedding-parallel sideritic hard-bands characterized variously either by sparse interstitial extremely fine siderite crystals or crystal-clusters (e.g. in the Murta Member of the Mooga Formation) or by more coarsely crystalline and more pervasive (including grain-replacing) versions of this pattern occur both in the Cadna-owie and Wallumbilla Formations (Fig. 8E,F; see also Etheridge et al., 1986, fig. 3). Additionally, the Cadna-owie Formation contains sideritic hard-bands characterized by more complex stellate cementation fabrics (Fig. 9A,B). Calcite-cemented hard-bands make their first stratigraphic appearance in NSW in the very top of the lacustrine Murta Member of the Mooga Formation (Etheridge et al., 1986, fig. 3) and are characterized by very coarsely crystalline poikilotopic calcite (with ferroan-calcite edges where in contact with detrital grains) preferentially developed in the coarse-grained laminae (Fig. 8A,B), interlaminated quartz siltstone in the same thin-section containing, contrastingly, sporadic ankerite pore-fillings. This circumstance suggests a porosity and permeability control on the growth of the two different minerals side-by-side, but the presence of pre-calcite quartz-overgrowths in the same rock (Fig. 8A,B) proves that the carbonate cements, though probably early on the basis of other cement-stratigraphy evidence, were not the first to have formed there. Ambrose et al. (1982) describe a similar cement stratigraphy for the Murta Member of the Mooga Formation in the adjacent deeper part of the basin in South Australia, where calcite cement is present more generally throughout the Murta Member and where it, similarly, post-dates quartz-overgrowths. In Lake Stewart 1, one hard-band of finely crystalline poikilotopic calcite in the Cadna-owie Formation (at 745.5 m depth) contains small isolated siderite rhombs or clusters of rhombs within the poikilocrysts, suggesting that the siderite pre-dates the calcite.

Calcitic hard-bands and concretions, many of the former with cone-in-cone structure, become more prevalent in the paralic upper part of the Cadna-owie Formation and in the overlying shallow-marine Wallumbilla Formation, the hard-bands attaining thicknesses up to 0.7 m and the concretions attaining diameters up to 2 m (Byrnes, 1984). Hard-bands of fibrous calcite, typically 10–15 cm thick, in which the fibres are arranged orthogonally to bedding also occur, and are interpreted by Byrnes (1984, p.139) to be the precursor of the cone-in-cone layers and to manifest "diagenetic expansive growths, rather than recrystallization products of calcareous beds". Byrnes (1984, p.139–140) cites textural evidence in support of this conclusion as well as for his conclusion that the calcitic and sideritic hard-bands "indicate an early diagenetic origin". Other calcitic hard-bands are described

by Byrnes (1984, p.139) as being "massive", comprising calcite-cemented sandstones in which the calcite crystals are not fibrous. In our experience, this latter variety of calcitic hard-band consists of relatively fine-grained sandstone characterized by pervasive granular to poikilotopic ferroan-calcite and minor associated calcite and ankerite (Fig. 9C). Feldspars and other labile grains are extensively replaced in such situations and porosity and permeability almost totally eliminated. Dolomite is not evident in the Cretaceous strata except possibly for one instance in the Cadna-owie Formation in Weilmoringle 1A where it occurs interstitially as sporadic rhombs associated with more pervasive siderite cement (Fig. 9B).

In thin-sections, crystals of the ferroan-carbonate cements of the Cadna-owie and Wallumbilla Formations commonly contain small pyrite framboids and/or cubic crystals in interstitial (non-grain-replacive) locations (cf. captions to Figs 8E,F, 9C) suggesting that the carbonate post-dates the iron-sulphide and hence is a product of the nonsulphidic, methanic environment (cf. Berner, 1981).

The overall scarcity of carbonates in the Jurassic fluvial strata and their progressive upsequence increase in relative abundance and mineral diversity through the Lower Cretaceous lacustrine, paralic, and shallow-marine strata (Table 5), taken together with the textural evidence that the carbonate cements are likely of early diagenetic origin, suggests that this pattern manifests the controlling influence of depositional environment and connate pore-fluids. Thus, the Jurassic fluvial sandstones contain only siderite, probably of pedogenic origin, and very rare dolomite; the overlying Lower Cretaceous lacustrine-to-paralic sandstones (Cadna-owie Formation and Murta Member of the Mooga Formation) have predominantly siderite but also some calcite (cf. Byrnes, 1984, p.140; Etheridge et al., 1986, fig.3) and possibly very rare dolomite, and the paralic and shallow-marine Wallumbilla Formation has predominantly ferroan-calcite and subordinate siderite. The prevalence of post-iron-sulphide ferroan-carbonates in the paralic and shallow-marine strata and their association with organic-rich mudrocks, especially in the Wallumbilla Formation, suggest that they are the product of methanic diagenesis (cf. Berner, 1981; Gautier, 1982; Gautier & Claypool, 1984) and as such are eogenetic (cf. Schmidt & McDonald, 1979a) carbonates. Because the development and persistence of the methanic diagenetic environment at shallow burial depth is largely a function of rapid passage of large quantities of reactive metabolizable organic matter through the successive microbial zones of aerobic oxidation and sulphate reduction, and because this is in turn enhanced by high sedimentation rates (cf. Gautier, 1982; van der Weijden, 1992), the carbonate hard-bands and concretions of the Cadna-owie and Wallumbilla Formations very likely manifest periods of accelerated clastic influx and accumulation, already estimated to be as high as 80–100 m/m.y. in the Wallumbilla Formation on the basis of radiometric dating of glauconie throughout this interval (Byrnes et al., 1975, table 2).